# PV GRID CONNECTED SYSTEM MODELING AND PERFORMANCE IN DHAHRAN ENVIRONMENT

BY

**FAHAD IBRAHIM BOUSBAIT**

A Thesis Presented to the
DEANSHIP OF GRADUATE STUDIES

**KING FAHD UNIVERSITY OF PETROLEUM & MINERALS**

DHAHRAN, SAUDI ARABIA

In Partial Fulfillment of the
Requirements for the Degree of

# MASTER OF SCIENCE

In

**ELECTRICAL ENGINEERING**

**December 2015**

KING FAHD UNIVERSITY OF PETROLEUM & MINERALS

DHAHRAN- 31261, SAUDI ARABIA

**DEANSHIP OF GRADUATE STUDIES**

This thesis, written by **Fahad Ibrahim Bousbait** under the direction his thesis advisor and approved by his thesis committee, has been presented and accepted by the Dean of Graduate Studies, in partial fulfillment of the requirements for the degree of **MASTER OF SCIENCE IN ELECTRICAL ENGINEERING.**

Dr. Mahmoud Kassas
(Advisor)

Dr. Ali Ahmad Al-Shaikhi
Department Chairman

Dr. Belhaj A. Chokri
(Member)

Dr. Salam A. Zummo
Dean of Graduate Studies

Dr. Ali Al-Awami
(Member)

27/12/15

Date

*Dedication*

I dedicate this work to my brothers, parents, sisters, my wife and my children

# ACKNOWLEDGMENTS

In the name of Allah, the most Merciful and the most Gracious. The one who has power overall. Peace be upon our prophet Mohammad Bin Abdullah, his family member, his groups, and all whom followed him till the Day of Judgment.

I am greatly thankful to my thesis advisor Dr. Mahmood Kassas for his usual support, inspiration and direction in successfully completing this work. I am indebted to his time, endurance and in appreciated suggestions that he gave in this thesis work. I would direct my genuine appreciation towards him.

I would also express my appreciations to my thesis committee members, Dr. Chokri Belhaj and Dr. Ali Al-Awami for their assistance and participation and time they secure to review and support my work.

I would also appreciate my parents, sisters, brothers and my wife for their endless support, love, endurance and prayers without which I may not be able to complete such great work. They have always been the basis of motivation for my achievement.

Finally, I would also thank Power Systems management of Saudi Aramco for providing me the time and resources for completing this study, specially my direct supervisor Eng. Mohammed Al-Zuabi and my colleague Eng. Toral Tulga.

# TABLE OF CONTENTS

# LIST OF TABLES

# LIST OF FIGURES

# ABSTRACT


Full Name : Fahad Ibrahim Bousbait

Thesis Title : PV Grid Connected System Modeling and Performance in Dhahran Environment

Major Field : Electrical Engineering

Date of Degree : December 2015



In this thesis, a time variant model of a constructed photovoltaic grid connected system in Dhahran area is developed and the effect of the actual solar panel temperature, dust accumulation and the fluctuation of the sun's irradiation on the performance of the system are investigated. The development of the model in accordance to the available online data from the constructed photovoltaic system is analyzed. Matlab®/Simulink® software is used to implement the model and obtain the simulation results.

The obtained results demonstrate the effect of the parallel resistor on the system performance. In this work, a proposed formula that includes irradiation, temperature and the load resistance factors towards the parallel resistor value is demonstrated and explained.

# ملخص الرسالة

**الاسم الكامل**: فهد إبراهيم بوسبيت
**عنوان الرسالة:** تصميم وتحليل لنظام طاقة شمية متصل بالشبكة الكهربائية في منطقة الظهران
**التخصص:** هندسة كهربائية
**تاريخ الدرجة العلمية**: ديسمبر 2015

تتناول هذه الرسالة تصميم نموذج كهربائي هندسي متغير زمنيا لنظام طاقة شمسية متصل بالشبكة الكهربائية في منطقة الظهران. كذلك تتضمن الرسالة دراسة للتغيرات المناخية في منطقة الظهران على انتاج الطاقة الشمسية. من هذه التأثيرات الغبار، الحرارة والتغيرات في الاشعاع الشمسي. تم تصميم النظام بناء على المعلومات والبيانات التي تم جمعها من مشروع لنظام طاقة شمسية تم تنفيذه في منطقة الظهران. تم تصميم النموذج باستخدام برنامج ماتلاب/سميولنك لتنفيذ التصميم وتحليل البيانات.

تشرح الرسالة تأثير المقاومة المتوازية في التصميم الكهربائي على أداء نظام الطاقة الشمسية. كذلك تقترح الرسالة معادلة جديدة لإيجاد قيمة المقاومة المتوازية باستخدام قيم الاشعاع الشمسي، الحرارة، والأحمال الكهربائية.

# CHAPTER 1

# INTRODUCTION

## 1.1 Overview

Photovoltaic cells convert most of the solar irradiation energy to electrical energy and some gets reflected to heat. This heat negatively affects the efficiency of the solar cell power output [1-2]. The energy conversion is simple but involves sophisticated technology to construct efficient devices, called solar cells, which are the main parts of a photovoltaic system [3]. Initially, the solar cells were found for the application of satellite power and only small amount of power was obtained. Later, a lot of technologies have been developed in solar cell manufacturing and were used for home and commercial applications [4].

Most of the applications require several series and parallel solar cells to produce sufficient voltage and power. These electrically connected cells are usually named as a module. The modules also protect individual cells from environmental conditions, were they are placed in between a single or double glasses. The same current will flows in series connection but the voltage the ends of the series is the sum of each cell voltages. However, to have all cells operate in maximum power point, it is very critical to match the series string of cells. Moreover, the parallel connection will produce a current equal to the sum of each cell currents [3].

The sunlight radiation that reaches earth surface, will be distributed over a range of wavelengths that start from 300 nm to 4 micron. Manufacturer's datasheets usually have the performance and the characteristics of the modules with admiration to the standard test condition (STC). This STC requires to have the test under constant irradiation level of 1000 W/m2, air mass coefficient of AM1.5 and a uniform fixed temperature at 25◦C [3]. An accurate model of a photovoltaic system is very important for power electronics engineers to guarantee the accuracy of the designs tested for performance using simulations.

Nowadays, power delivered by the solar cell is increased by adopting new techniques. Some techniques have different material properties, and others using various PV array topologies. The PV modules lifecycle after installation is expected to perform up to 20 years. However, the environmental aspects, high irradiation and high temperature will affect the performance of PV modules. Moreover, integral internal manufacturing defects could affect the performance of PV modules [4].

## 1.2 Thesis Motivation

Due to the summer temperature of more than 40 degree centigrade and the dusty seasons here in Dhahran area in Saudi Arabia, a number of problem come up with the large installation of PV panels. All these problems contribute to the total generated power to the grid.

Thus, analyzing the impact of temperature, dust accumulation, fluctuation of the sun's irradiation on the PV system performance and proposing a mathematical solution adds countless value to Photovoltaic modeling research field. Moreover, this work will validate the design parameters of the PV system operated in harsh environment here in Dhahran area.

## 1.3 Thesis Objectives

- Development of a Photovoltaic time variant model using Matlab®/Simulink® that will include solar irradiation and module temperature as well as the dust accumulation.
- Studying the power performance of the PV system considering the environment parameters in Dhahran area.

# CHAPTER 2

# LITERATURE REVIEW

## 2.1 Photovoltaic Physics

Photovoltaic cells operation is based on the photoelectric effect. That is based on the release of the electrons from the surface of photovoltaic material when sunlight hit that surface. As much as the numbers of photons are available the numbers of escape electrons are increased, that is, the intensity of sunlight, and energy of electrons are governed by on the energy of photons [5-7].

However, only when there is a voltage difference, the generation of electricity is possible. The mobile electrons will travel in a desired manner through the p-n junction diode which contains two types of semiconductors.

## 2.2 The p-n junction

When these type of semiconductors p and n are in contact at the area of the junction line, the electrons diffuse from the n side to the p side. In addition they will combine with the holes. This will create fixed negative ions at the p side and keep positive ions at the n side. Therefore, an equilibrium is achieved with no other diffusion.

The junction at the diode is divided into two areas: the depletion area and the quasi-neutral area. Figure 1 shows the diffusion and the depletion layer where the depletion area containing the junction area.

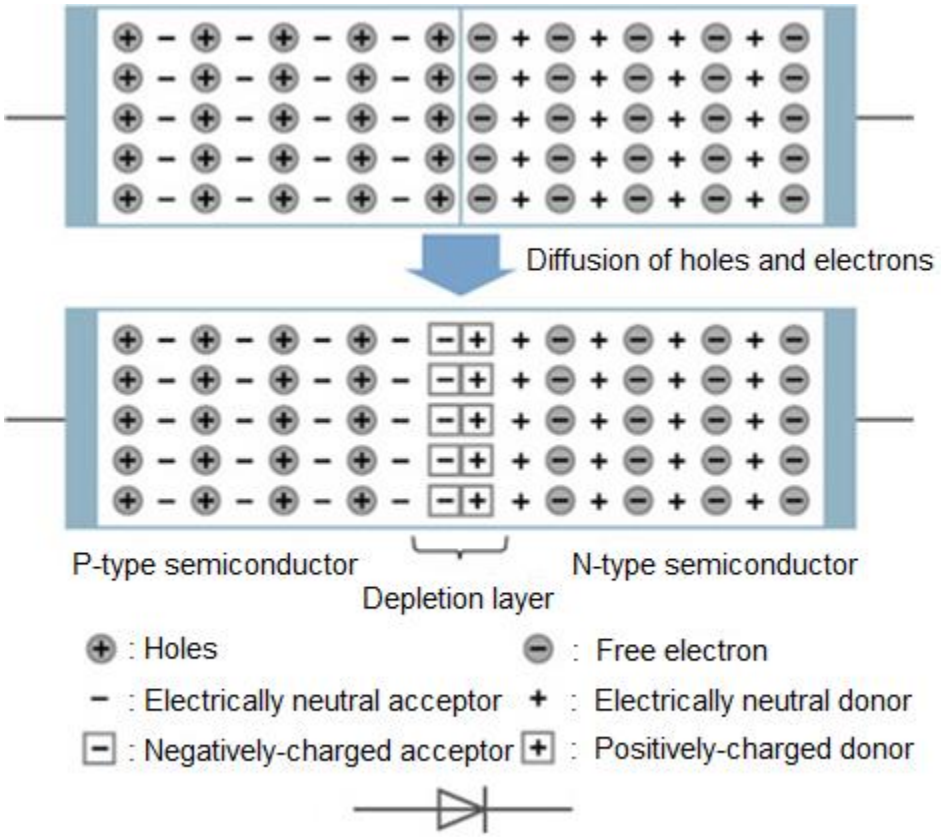


**Figure 1: The p-n junction.**

## 2.3 Types of Photovoltaic Cells

Photovoltaic cells have two main types:

### 2.3.1 Polycrystalline Silicon Cell

Polycrystalline silicon (polySi) is collective of many ounces of single-crystal silicon. Both quality and the size of the ounces enhance the solar performance: more perfect

ounces and larger ones provides electric behavior that will be similar to a cell constructed from single-crystal silicon [5].

### 2.3.2 Amorphous Silicon Cell

These silicon cells have an atomic structure that is different from the polycrystalline as it is not in order. In early stage, amorphous silicon material was considered to be unsuitable for PV industry since it has different structural and electrical properties [5-7]. Lately, by properly controlling the conditions of depositing and by wisely adjusting the composition, amorphous silicon has become ready to be used for solar cells. Moreover, the future of PV power generation through direct sunlight is moving toward the amorphous silicon cell.

## 2.4 Mathematical Model for Photovoltaic Cell

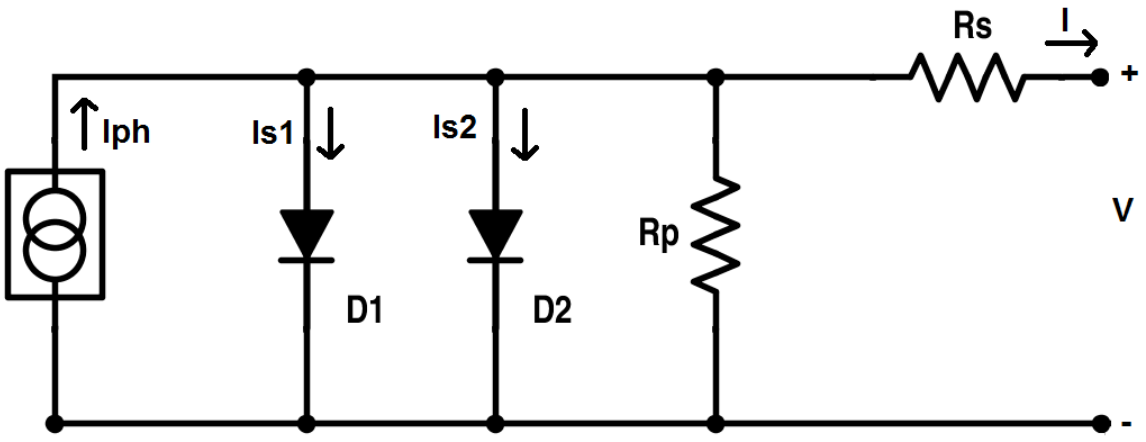


**Figure 2: Double diode model for solar cell.**

This model has a current source $I_{ph}$, two diode, series resistance and a parallel resistance as shown in figure 2 [9-16]. The net current $I$ is the difference between the photocurrent $I_{ph}$ and the sum of the normal diode current $I_{s1}$, $I_{s2}$ , and the current through $R_p$. Therfore, the characteristic equation (1) of the above solar cell is mathmaticaly given as:

$$.I = I_{ph} - I_{s1}\left[e^{\left(\frac{q(V+IR_S)}{KTA_1}\right)} - 1\right] - I_{s2}\left[e^{\left(\frac{q(V+IR_S)}{KTA_2}\right)} - 1\right] - \frac{(V+IR_S)}{R_p} \quad (1)$$

Where:

K= Boltzmann Constant $1.38*10^{-23}$ J/K

$A_1$ = Ideal factor for the first diode.

$A_2$ = Ideal factor for the second diode.

T = Temperature in fehrenhite.

However the double diode model can be further simplified by deleting the current $I_{s2}$ -the reverse saturation current of diode *D2*. This is due to recombination of charge carrier in space charge layer is negligible. This assumption is very much acceptable considering the standard test conditions [10]. Hence, the comprehensive model of the solar cell with single diode is shown below in Figure 3 and is mostly used for analytical and design purposes with acceptable accuracy [6-7] and [17-28]. The single diode model equation is presented in equation (2).

$$\mathrm{I} = I_{ph} - I_{s1}\left[e^{\left(\frac{q(V+IR_S)}{KTA_1}\right)} - 1\right] - \frac{(V+IR_S)}{R_p} \quad (2)$$

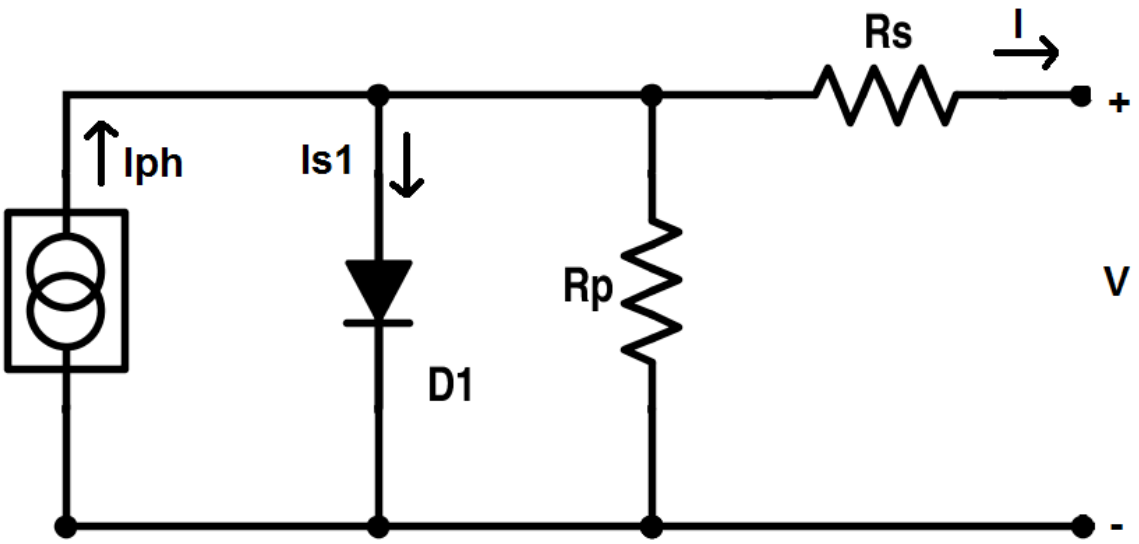


**Figure 3: Single diode model for solar cell.**

Both double and single diode model for solar cell are temperature dependent. Equations (3-8) illustrate the different relation with temperature [7], [15-16], [18], [21-22], [25] and [28]:

$$I_{ph}\,(\mathrm{T}) = I_{phn}\,(\,1 + K_I\,(\,\mathrm{T} - T_0\,)\,) \tag{3}$$

$$V_{oc}\,(\mathrm{T}) = V_{ocn}\,(\,1 + K_V\,(\,\mathrm{T} - T_0\,)\,) \tag{4}$$

$$I_s\,(\mathrm{T}) = I_{sn}\,(\frac{T}{T_0})^{(\frac{k_1}{A_1})}\;\; e(\frac{E_g(\frac{T}{T_0}-1)}{(A_1\,v_t)}) \tag{5}$$

$$I_{sn} = \frac{I_{sc}}{e^{\left(\frac{V_{oc}}{A\,V_t}\right)}-1} \tag{6}$$

Where:

$V_t = \frac{KT}{q}$ ; Thermal voltage

$V_{oc}$ = Voltage at no load (open voltage)

$I_{sc}$ = Short circuit current.

$V_{ocn}$ = Nominal open voltage

$I_{phn}$ = Photovoltaic nominal generated current

$I_{sn}$ = Diode nominal saturation current

$E_g$ = The solar cell activation energy

$K_I$ = Short circuit current coefficient (A/K)

$K_V$ = Open circuit voltage coefficient (V/K)

$T_o$ = Nominal temperature

$k_1$ = Temperature exponent for first diode

Considering the variation in Irradiation, equation 3 can be improved by the following equation [7], [15-16], [20-23], [25] and [28]:

$$I_{ph}\,(\mathrm{T}) = I_{ph}\,(\,1 + \alpha\,(\,\mathrm{T} - T_0\,)\,)\,\frac{G}{G_n} \qquad (7)$$

As the $I_s$ is strongly dependent on temperature, the saturation current in equation 5 can be improved by the following [20] and [23]:

$$I_s = \frac{I_{sc} + K_I\,\Delta T}{e^{\left(\frac{V_{oc} + K_V\,\Delta T}{A\,V_t}\right)} - 1} \qquad (8)$$

# CHAPTER 3

# SYSTEM MODELING

## 3.1 System Description

The target system is constructed in Dhahran with a design capacity of 10.5 MW. This system is composed of two main substations with similarity in design and equipment where each is designed for 5.25 MW. Each substation has eight subsystems. Each subsystem is made of amorphous PV modules, one central box, one inverter and one grid connected transformer. Figure 4 shows single line diagram of substation 1.

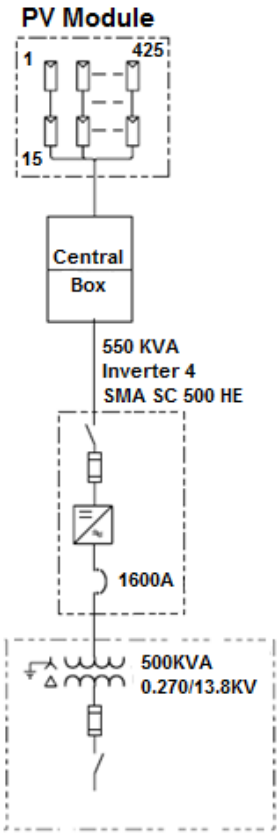


**Figure 4: One PV subsystem.**

### 3.1.1 PV modules

A total of 125858 modules are installed for this project. 62528 panels for substation 1 and 63330 for substation 2. Different PV module ratings are used to comply with the available area and the total equivalent voltage. Moreover, the PV modules are connected in parallel and series to match the voltage level and the inverter rating. Table 1 shows the PV ratings:

**Table 1: Installed PV Modules**

| Module Model Number | Vmax (V) | Imax (A) | Pmax (W) | Total Number | Total Power (W) |
|---|---|---|---|---|---|
| SC-70 EX-A | 37.6 | 1.85 | 70 | 6664 | 466480 |
| SF-75 EX-B | 40.5 | 1.85 | 75 | 19924 | 1494300 |
| SF-80 EX-B | 41 | 1.95 | 80 | 15090 | 1207200 |
| SF-82 EX-B | 41.7 | 1.98 | 82.5 | 8820 | 727650 |
| SF-85 EX-B | 42.5 | 2 | 85 | 35745 | 3038325 |
| SF-87 EX-B | 43.8 | 2 | 87.5 | 21615 | 1891312.5 |
| SF-90 EX-B | 45 | 2 | 90 | 18000 | 1620000 |

### 3.1.2 Central Box

The central box is used for the following reasons:

- To combine all DC cables at one bus.

- To record the DC voltage and current for each individual parallel and series section.
- To maintain each section as needed for maintenance purposes.

### 3.1.3 Inverter

Two different Inverters are used for this project i.e. SC-630HE-20 and SC-500HE-20. The main difference is the power rating. The below table 2 shows the inverters ratings:

**Table 2: Installed Inverters**

| Inverter Model | Nominal Inverter Rating (kW) | Total Number | Total Power (kW) |
|---|---|---|---|
| SC-630HE-20 | 630 | 10 | 6300 |
| SC-500HE-20 | 500 | 8 | 4000 |

### 3.1.4 Transformer

Two different transformers are used for this project. Both are selected based on the inverter rating and the total PV modules. Table 3 shows the installed transformer ratings:

**Table 3: Installed Transformers**

| Transformer Nominal Rating (kW) | Total Number | Total Power (kW) |
|---|---|---|
| 750 | 13 | 9750 |
| 500 | 5 | 2500 |

## 3.2 Selected Subsystem

Since the full system consist of similar subsystems with individual monitoring and control, one complete subsystem was selected for this thesis study. The subsystem consist

of 6345 PV panels, one control box, one inverter and one transformer. Also, as the transformer secondary is connected directly to the 13.8KV grid, and the inverter is coupled directly to the transformer, they were not considered in the modeling and analysis for this thesis study. The scope of this study will focus on the modeling and environmental analysis of the PV panels including the DC cables connections up to the inverter input. The following sections discuss in details the PV panels with DC cables modeling. .

## 3.3 The Photovoltaic Module

PV module consist of a mixture of parallel and series individual solar cells. Also, additional elements of bypass and blocking diodes are added. Generally, the single cell voltage handling ability is around 0.6V. Manufacturers produce solar modules in order to have higher voltage and current capabilities. This is achieved by grouping solar cells in parallel and series connections. The series connections will manage the voltage level and the parallel connections will manage the current level. A diversity of connection arrangements exist in the industry, however, a common arrangement for a grid connected system is with 72 series cells. For example, the Solar Frontier K. K. SF80-EX-B module used in this study provides rated voltage of 41V and 1.95 A.

Two assumptions generally are used for PV design and modeling:

1- The series connections will be responsible of increasing the system voltage and the parallel connections will be responsible increase the system current.

In this assumption all solar cells will perform in a uniform way, however, this is not always true. Photovoltaic modules contains bypass and blocking diodes that will reduce the effect of un-uniform cells. Without these diodes it is possible for the un-uniform cells to drain power generated by the other cells. For the purpose of modeling, the blocking and bypassing diodes are reflected as ideal diodes.

2- All cells behave uniformly within a given environmental states and each cell have the same electrical characteristics.

### 3.3.1 Bypass diode

They are located between each cell in a solar module and their purpose is to have the maximum possible voltage from each series string. This will protect the solar cell that does not have the same illumination as the others in the same string. As an example, in a given string, it is possible that single or multiple cells will be covered with dust and therefore absorbs less radiation. Then these cells voltage gain could have the possibility to reverse its direction which will result in a voltage reduction of the entire series string. Thus, the bypass diode will become forward biased and will create a short across the cell. Figure 5 shows normal and bypass modes for solar cells.

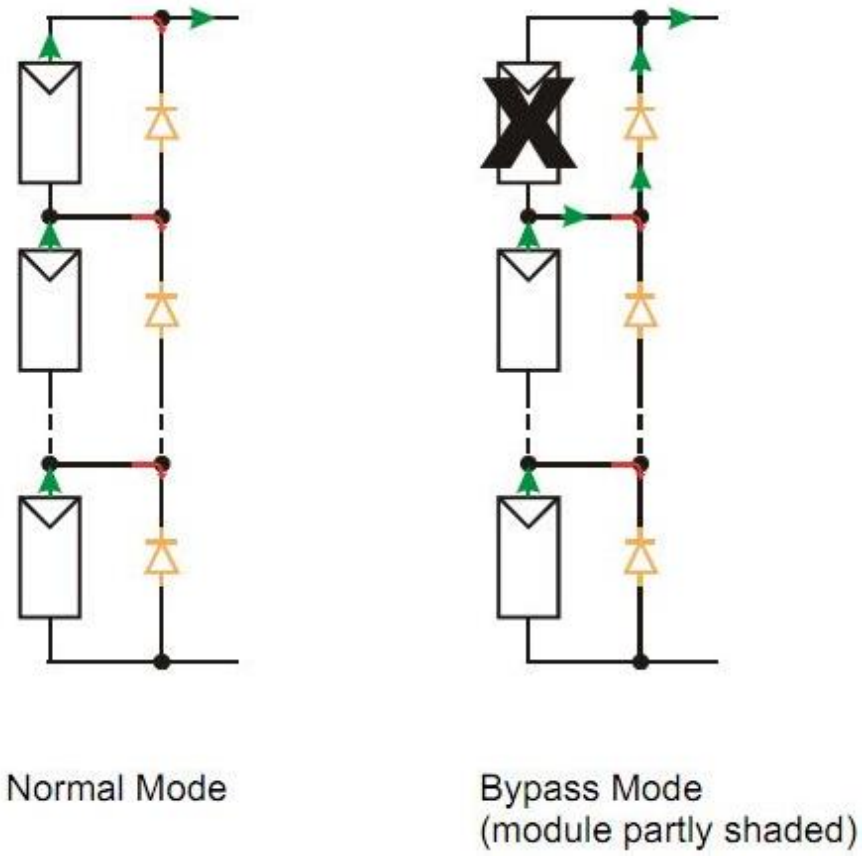


**Figure 5: Bypass diode.**

### 3.3.2 Blocking diode

These are located between each string series connections and the termination point to prevent the solar module from draining power from the connected system when not generating power. When zero radiation and availability of forward voltage provided by the connected system, a string will absorb current from the system circuit. These blocking diodes will also protect each module when connected with other modules to form an array. Figure 6 shows both bypass and blocking diodes.

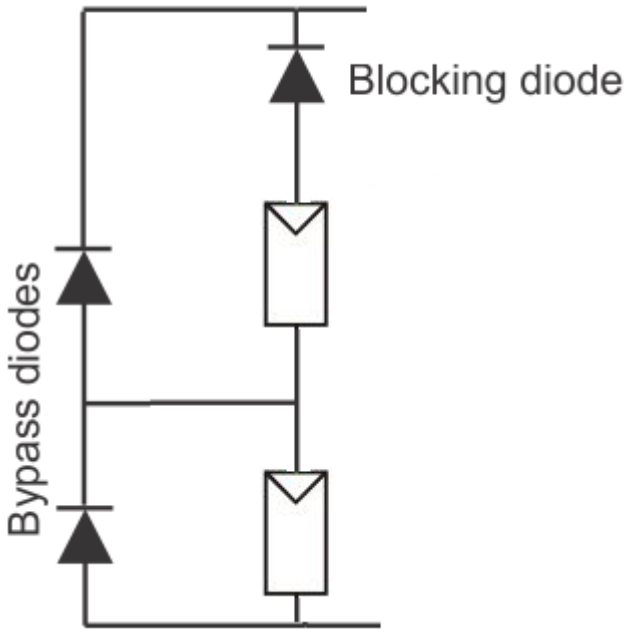


**Figure 6: Bypass and blocking diodes.**

## 3.4 The Photovoltaic Array

Photovoltaic array is a group of series and parallel photovoltaic modules connected together to generate the required voltage and current. The number of series modules will multiply the system voltage and the number of parallel modules will multiply the system current so that will produce the desired power output of the array. Therefore it is important for each string of solar modules to be collected of similar number of connected modules that have the same power rating. If the strings have different voltage levels, then the voltage output will be lower than other string voltage; thus the highest string voltage does not generate power at the design maximum efficiency. Figure 7 demonstrate cell, module, string and array.

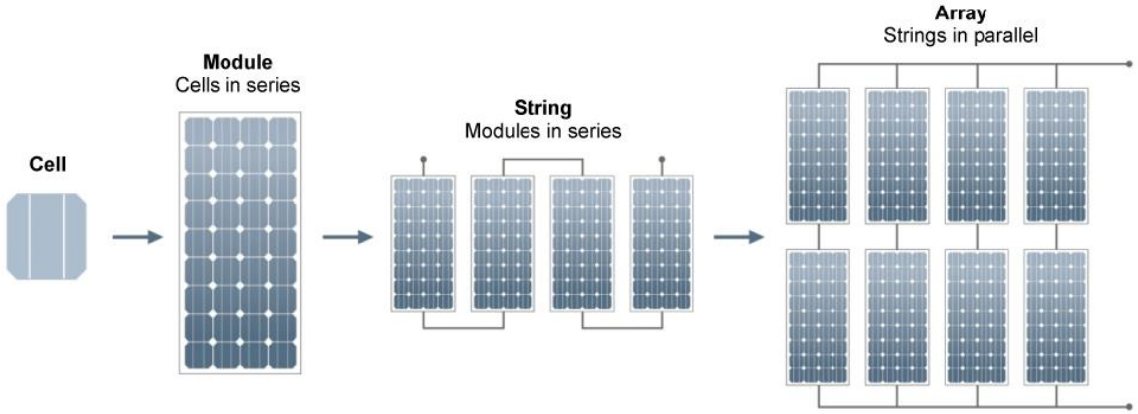


**Figure 7: Demonstration of Cell, Module, String and Array.**

Photovoltaic grid connected system has an inverter and a transformer. Usually the inverters operates at the largest possible rated DC voltage input and as an example for this thesis case it is 615V.

Solar modules equivalent circuit is organized in parallel $N_P$ and in series $N_S$ as explained in Figure 8. The mathematical model using single diode model is presented in equation (9).

$$I = N_p I_{ph} - N_p I_s \left[ e^{\left( \frac{(V + R_s \left( \frac{N_s}{N_p} \right) I)}{V_t A N_s} \right)} - 1 \right] - \frac{V + R_s \left( \frac{N_s}{N_p} \right) I}{R_p \left( \frac{N_s}{N_p} \right)} \quad (9)$$

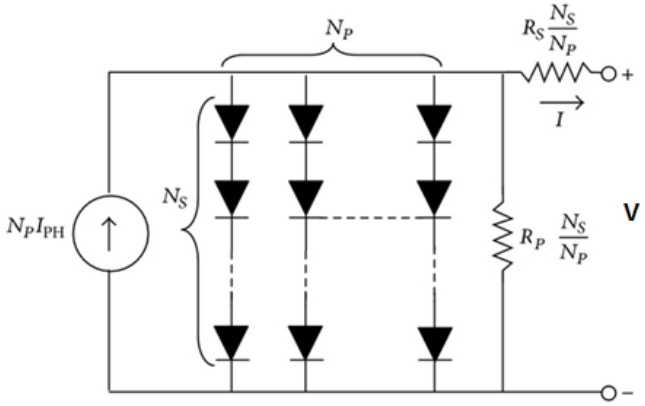


**Figure 8: General model of PV array.**

## 3.5 Solar Cell Module Mathematical Model

To develop the solar cell module mathematical model, it is necessary to get the manufacturer lab test results under controlled environmental conditions. These conditions are:

- Temperature = 25°C
- Irradiation = 1000 W/$m^2$
- Air Mass coefficient = 1.5 $L/L_o$

Were:

L = Path length through atmosphere.

$L_o$ = Zenith path length normal to earth's surface at sea level.

Figure 9 demonstrate air mass coefficient.

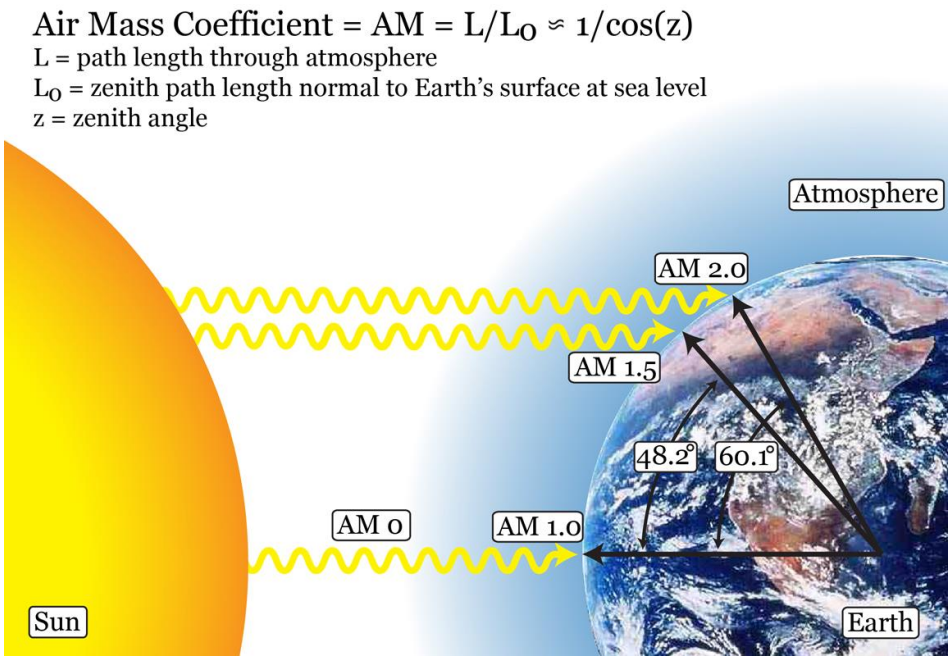


**Figure 9: Air mass coefficient.**

Also, it is necessary to get the module data sheet (SF80-EX-B) with basic parameters value. These parameters are presented in table 4.

**Table 4: Parameters of the SF80-EX-B solar module at 25°C, 1.5AM, 1000W/m$^2$**

| | |
|---|---|
| $V_{OC}$ | 58.43 V |
| $I_{SC}$ | 2.21903 A |
| $K_V$ | -0.0029 V/K |
| $K_I$ | 0.0003 A/K |

### 3.5.1 Single module curve fitting

Figures 10 and 11 demonstrate the constructed model using Matlab®/Simulink® to get all the design parameters through IV curve fitting compared to the manufacturer tabulated IV data. The model is constructed using equation (2) where the photovoltaic generated current ($I_{ph}$) subtracting the diode current is shown in equation 10.

$$I_m = I_{ph} - I_{s1}\left[e^{\left(\frac{q(V+IR_S)}{KTA}\right)} - 1\right] \qquad (10)$$

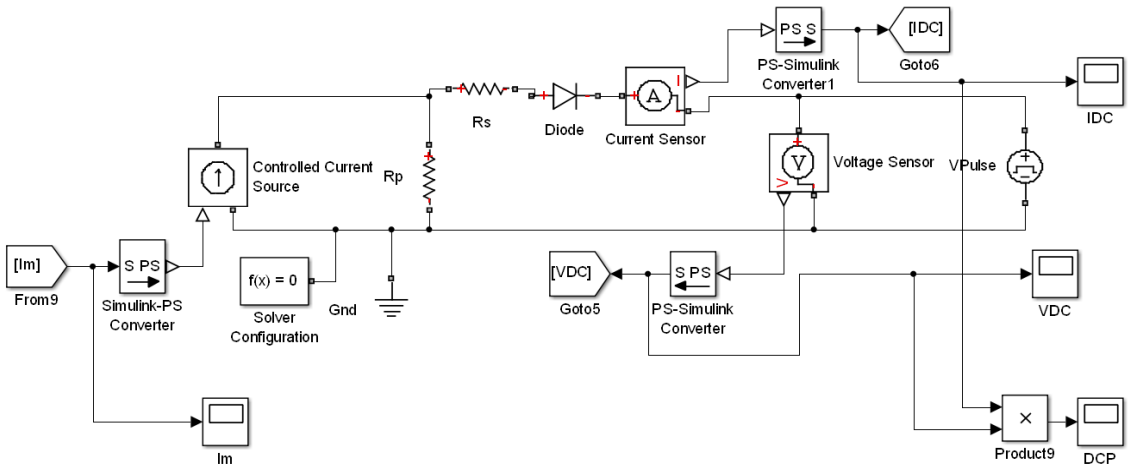


**Figure 10: Curve Fitting Model (part 1)**

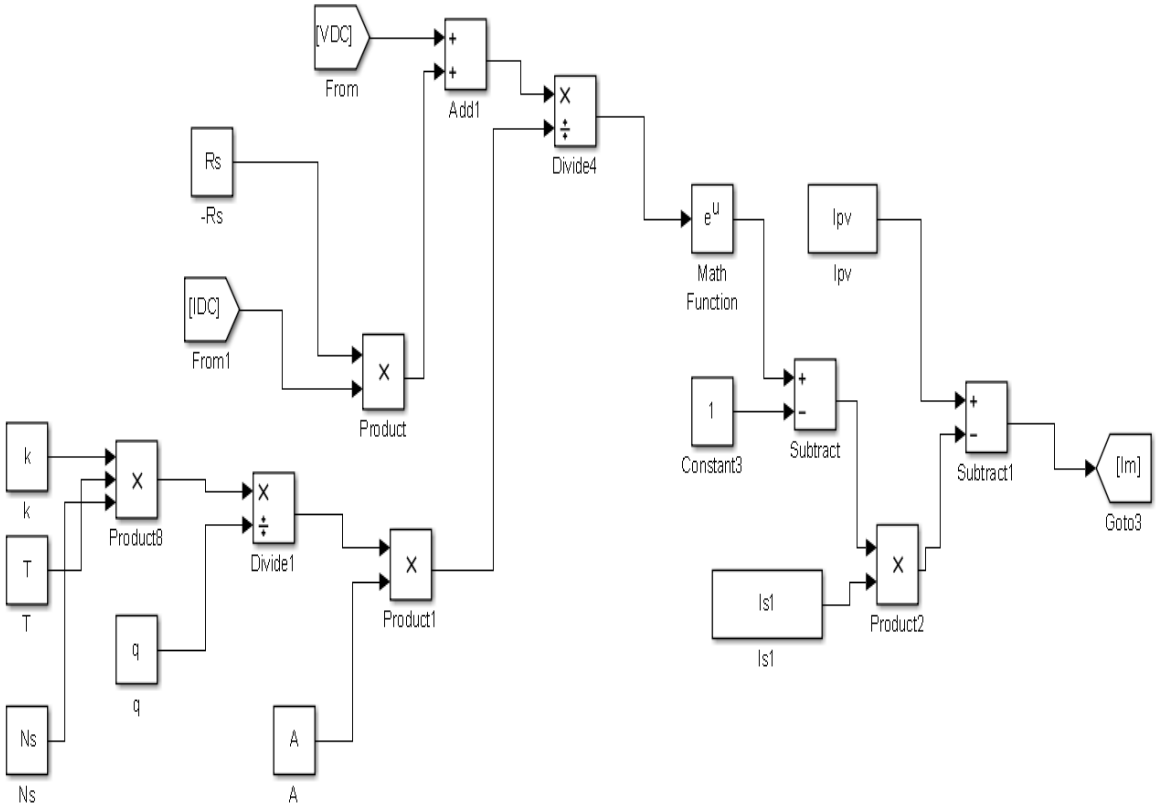


**Figure 11: Curve Fitting Model (part 2)**

The diode used after the series resistor is an ideal diode to overcome the reverse circulating current by the *VPulse* voltage generation unit. The *VPulse* is used to simulate the resistive load variation starting from short circuit load to an open voltage state. The model will monitor and record the generated current ($I_m$), load current (*IDC*), load voltage (*VDC*) and the total generated power (*DCP*) at the load side. Diode saturation current $I_{s1}$ is calculated using equation (8).

$$I_{s1} = \frac{I_{sc} + K_I \Delta T}{e^{\left(\frac{V_{oc} + K_v \Delta T}{A V_t}\right)} - 1} \qquad (11)$$

The unknown parameters are $R_s$, $R_p$, A, and $I_{pv}$ where (fminsearch) was used to find the optimum parameters value that will fit the test lab result with the model result.

The simplified flowchart of the iterative modeling algorithm is shown in figure 12.

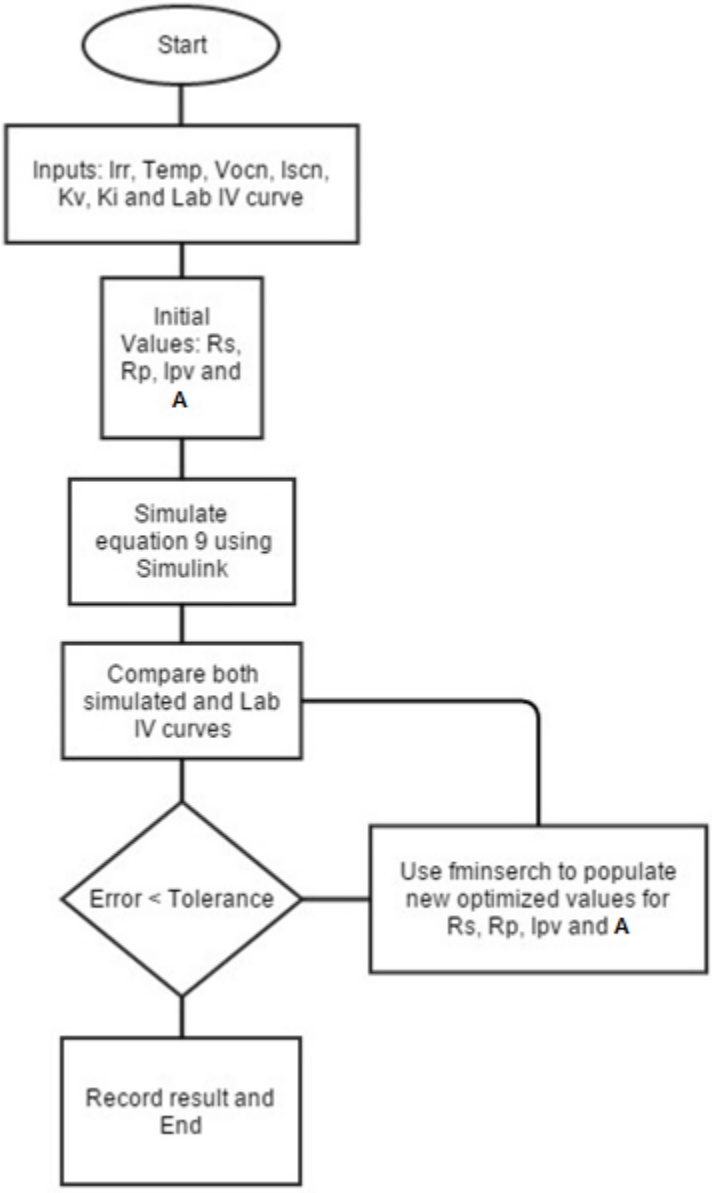


**Figure 12: Algorithm of the method used for curve fitting**

After several iterations, the tolerance value of $6.02*10^{-4}$ between the lab current data points and the simulation current data points was achived and the optimized parameters value are presented in table 5. Figure 13 shows the final curve fitting result.

**Table 5: Parameters of the fitted curve at nominal operating conditions**

| | | | |
|---|---|---|---|
| $V_{oc}$ | 58.43 V | $R_s$ | 5.0475 Ω |
| $I_{sc}$ | 2.21903 A | $R_p$ | 298.1150 Ω |
| $K_v$ | -0.0029 V/K | A | 96.3783 |
| $K_i$ | 0.0003 A/K | $I_{pvn}$ | 2.2640 A |
| k | $1.3807e^{-23}$ J/K | q | $1.6022e^{-19}$ C |

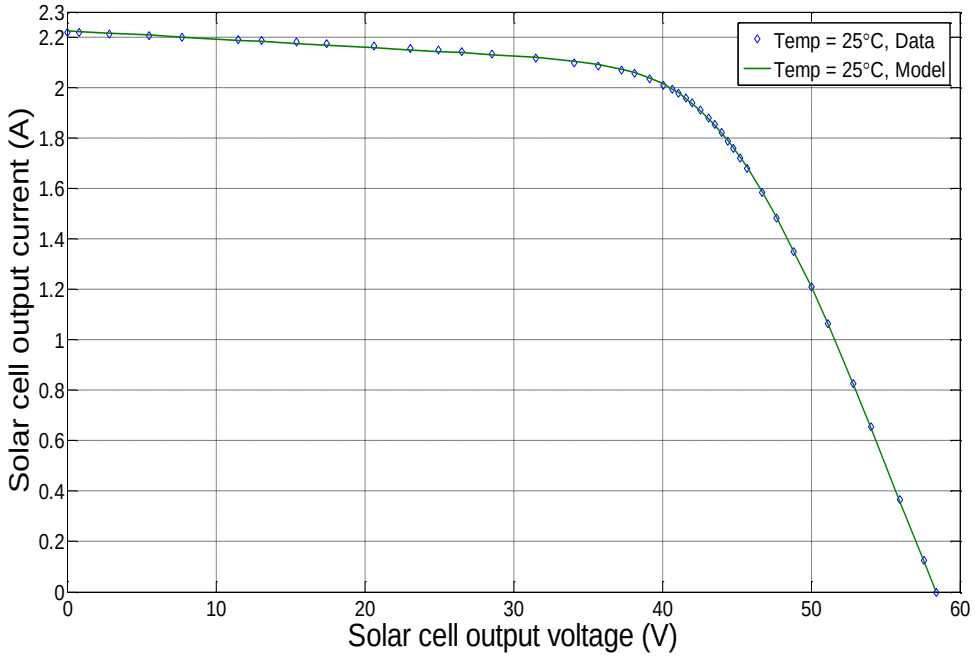


**Figure 13: IV Curve Fitting Result**

### 3.5.2 IV and PV single module curves

Since the module parameters are found, then IV and PV curves for different irradiation and temperature can be found. The irradiation was changed to different values (800, 600

and 400) keeping the temperature unchanged. Then the temperature was changed to different values (0, 50 and 75) keeping the irradiation unchanged. After that PV curve is calculated at the previous conditions. These are demonstrated in figures 14, 15, 16 and 17.

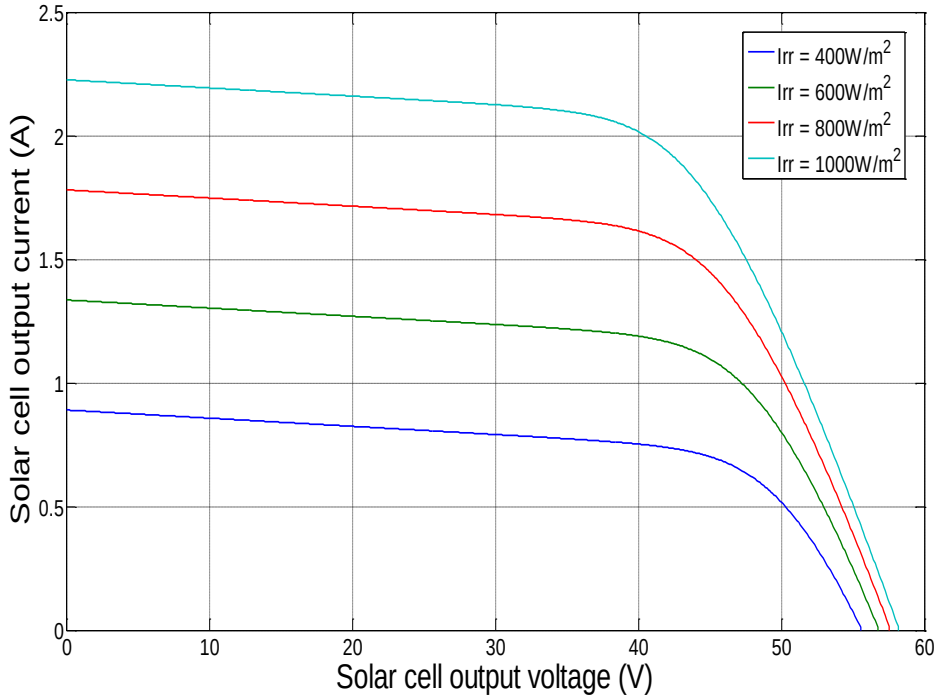


**Figure 14: IV curves with different Irradiation at 25°C**

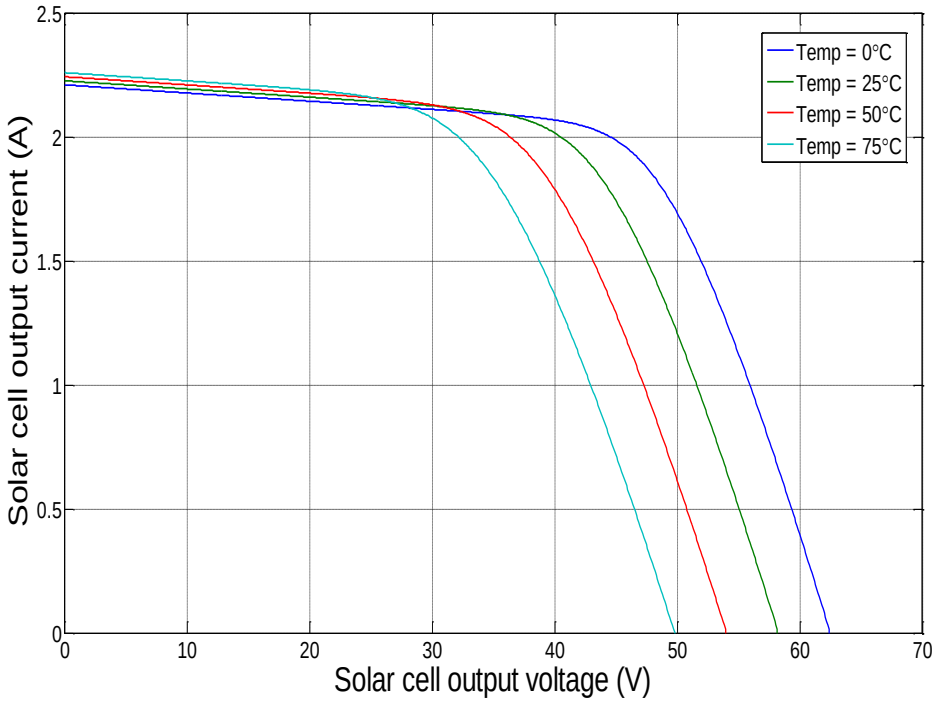


**Figure 15: IV curves with different temperature at 1000 W/m$^2$**

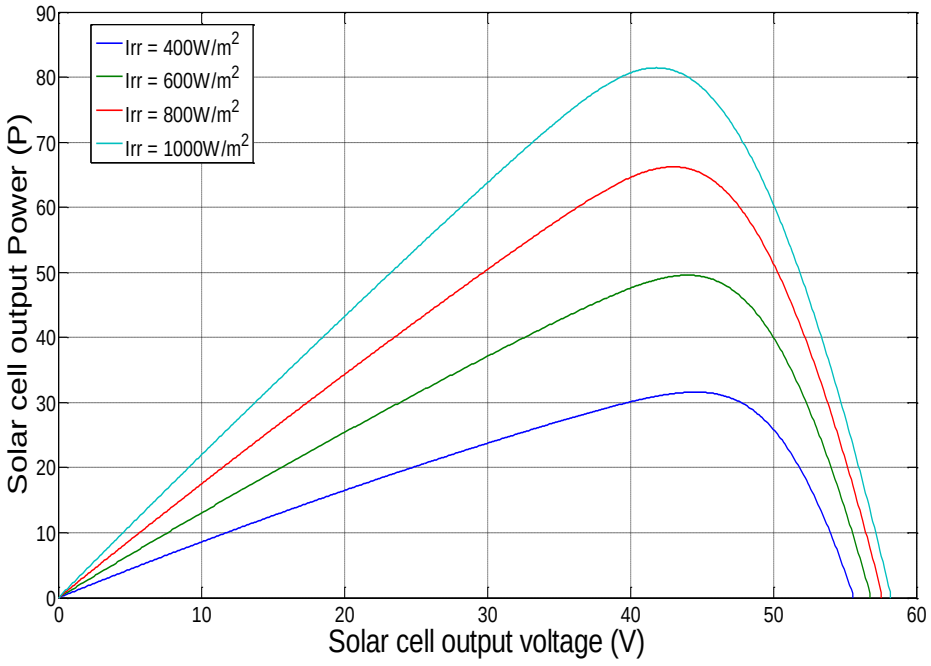


**Figure 16: PV curves with different irradiation at 25°C**

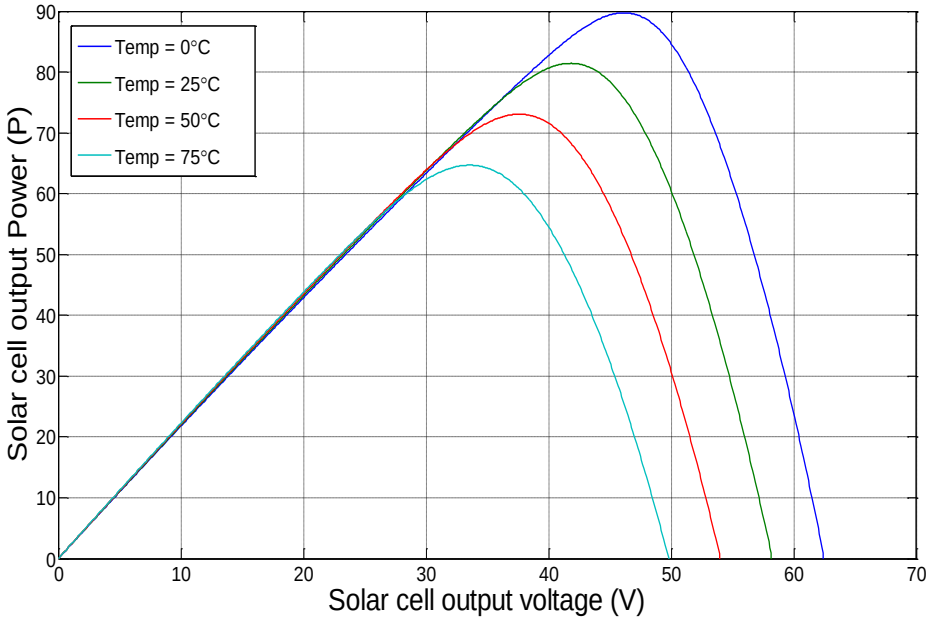


**Figure 17: PV curves with different temperature at 1000 W/m$^2$**

## 3.6 Photovoltaic System Mathematical Modeling

The selected system consist of seven main sections connected to the same central box with different cable length. And each section hold different photovoltaic arrays with common 15 modules in series and different parallel connections. Table 6 demonstrate the system modules connection with total number.

Since the system consist of large number of modules connected with parallel connections and cable lengths, the simulation of the system by Matlab®/Simulink® will take very long time. Therefore, the following assumptions were used to model the system:

**Table 6: Total number of modules**

| Section No | cable length - one way (m) | Count of series modules | Count of modules with 1 module in parallel | Count of modules with 2 module in parallel | Count of modules with 3 module in parallel | Count of modules with 4 module in parallel | Count of modules with 6 module in parallel | Total number of modules |
|---|---|---|---|---|---|---|---|---|
| 1 | 244 | 15 | | 2 | | | 5 | 510 |
| 2 | 210 | | | 2 | 1 | | 10 | 1005 |
| 3 | 222 | | | 2 | | 1 | 9 | 930 |
| 4 | 188 | | | 1 | 2 | | 10 | 1020 |
| 5 | 200 | | | 2 | | 1 | 9 | 930 |
| 6 | 166 | | 1 | | 3 | | 10 | 1050 |
| 7 | 178 | | | 3 | | | 9 | 900 |
| Total | | 15 | 1 | 12 | 6 | 2 | 62 | 6345 |

1- The irradiation received by each module is unified. This assumption is used as the irradiation value of each module is not measured. Also, considering the large number of connected modules, it is not economically justified to monitor each module irradiation value. However, the real system may receive slightly different irradiation values as, for example, they may contain different dust accumulation thickness.

2- Since each module is equipped with blocking diode, each module is considered as a current generation element. This assumptions is used to find the system equivalent resistor.
3- All Cable resistances are rated for fixed temperature of 45°C. This assumption is due to the summer average ambient temperature in Dhahran [1]. Moreover, the cable's temperature variation was not considered as most of cables were not exposed to direct sunlight.

Therefore, the following steps were used to construct the full system mathematical model:

1- Measure the cable length between each module and the branch cable.
2- Measure the cable length between each branch and the main cable connected to control box.
3- Collect all cable's data sheets.
4- Calculate cables resistant value.
5- Construct the full system module using Simulink® with all cable connections as shown in figure 18.
6- Construct the full system module without any cable connection as shown in figure 19.
7- Simulate both systems.
8- Calculate the total cables equivalent resistance by calculating the difference between both systems equivalent resistance at the maximum power output as shown in figure 20.

9- Construct the full system module with one equivalent module and one series equivalent resistance as shown in figure 21.

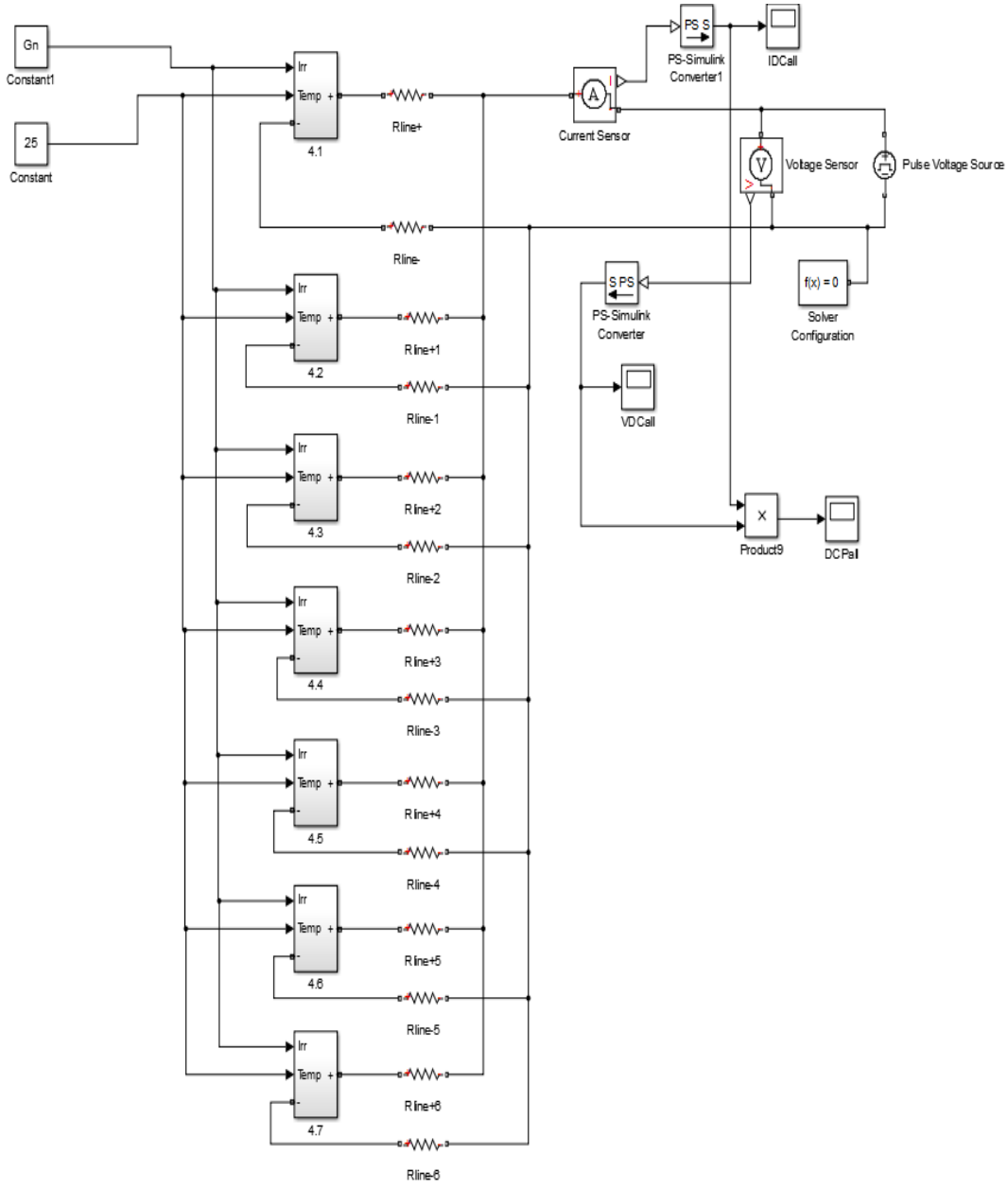


**Figure 18: Full system modeling with all resistors**

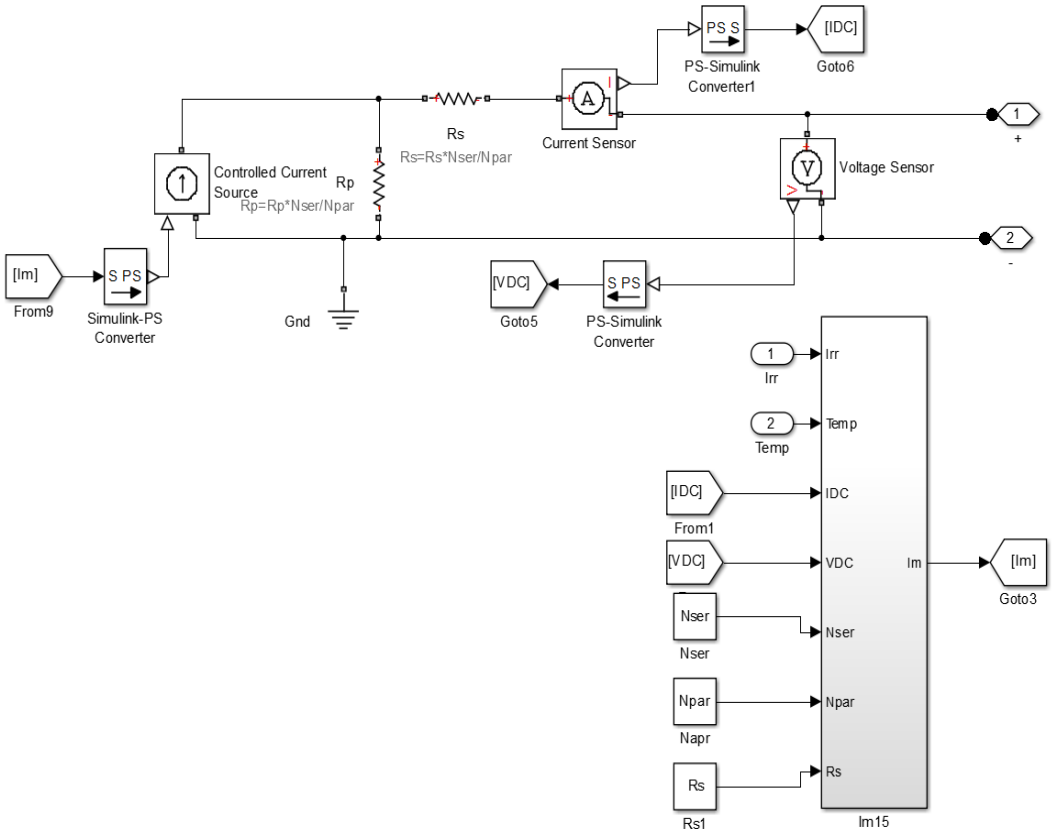


**Figure 19: Full system modeling without any line resistors**

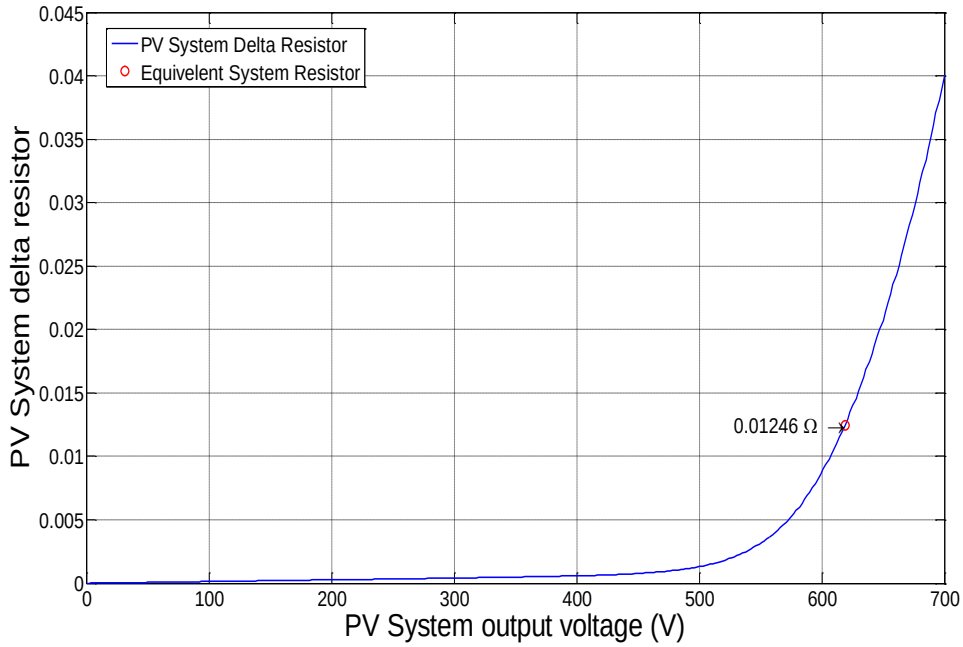


**Figure 20: PV system equivelant resistor**

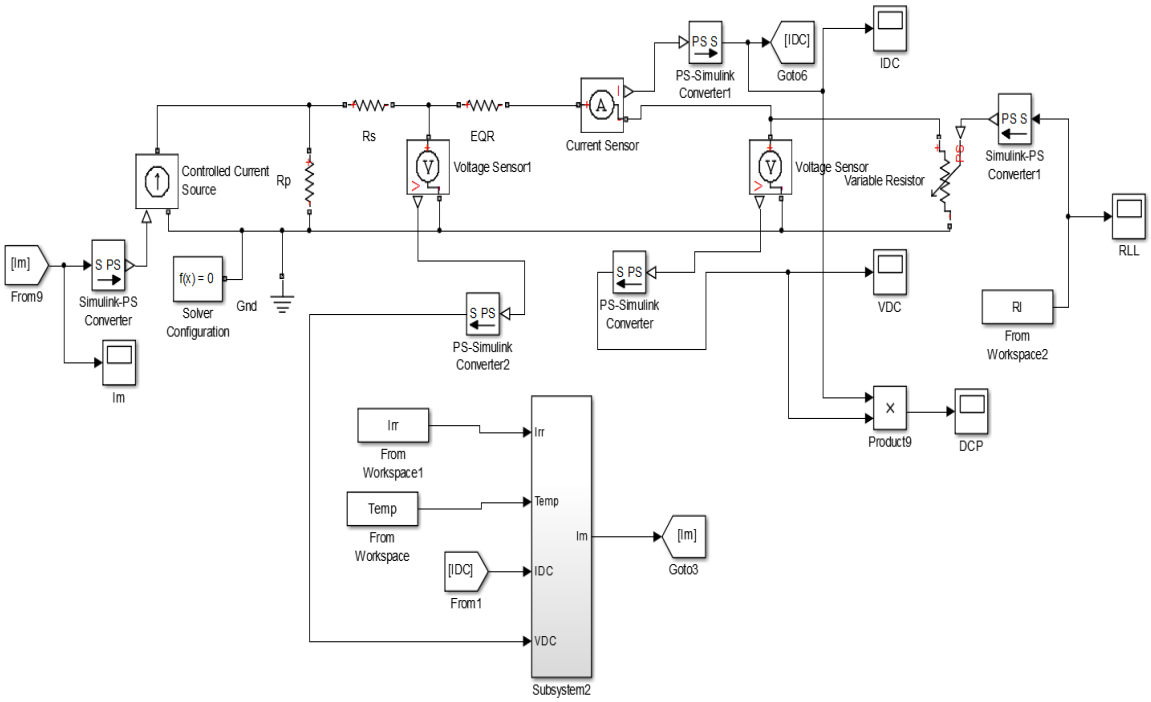


**Figure 21: Full system model with equivalent resistor**

## 3.7 Photovoltaic System Measured Data

Considering the scope of this work that includes the environmental analysis, it was necessary to record the system performance for a full year. The record period starts on 15 march 2013 and ended on 12 march 2014 with a total data size of 16 GB. However, due to some communication issues the following 23 days in 2013 were not recorded. These are 4 days in September (16-19) and 19 days in November (1-19).

Several individual sensors are used to record data. To illustrate, the selected system has the following sensors:

1- One irradiation sensor for the 6345 PV modules.

2- One PV module temperature sensor connected to one PV module in section 7.

3- Seven (7) DC current sensors located at the central box. One for each section.

4- One DC voltage sensor located at the main DC bus in the central box.

5- One ambient temperature sensor.

These sensors are connected to the main logger unit. The logger unit record these sensors value each second. In addition, 3 phase currents, 3 phase voltages, and AC power at the inverter secondary are recorded. However, the logger has a memory limitation that can record two months as a maximum and after that the new data will dominate. The logger file format is Microsoft Excel CSV file. It was necessary to prepare the file to a Matlab format. Hence, the following steps was followed:

1- Separate the date into day, month and year columns.

2- Separate the time into second, minute and hour columns.

3- Add the total DC current by the sum of each individual section.

4- Save the file in xlsx format with each day separately. The individual file contain 54000 lines as each day hold 15 hours of recorded data (1-second resolution).

After that, Matlab m file was developed using the following steps:

1- Convert the file from xlsx format to mat format.

2- Calculate the apparent power S.

3- Calculate the DC power.

4- Calculate the inverter losses.

5- Calculate the power factor.

6- Calculate theta in radian.

7- Calculate the reactive power Q.

The final mat file for each day contain in order 30 columns as follows:

1- Year

2- Month

3- Day

4- Hour

5- Minute

6- Second

7- DC current for section 1.

8- DC current for section 2.

9- DC current for section 3.

10- DC current for section 4.

11- DC current for section 5.

12- DC current for section 6.

13- DC current for section 7.

14- The sum of all DC currents.

15- Main DC voltage.

16- AC current phase a.

17- AC current phase b.

18- AC current phase c.

19- AC voltage phase a-b.

20- AC voltage phase b-c.

21- AC voltage phase a-c.

22- AC real power in Watt.

23- Modules temperature in °C.

24- Irradiation in $W/m^2$.

25- Ambient temperature in °C.

26- Apparent power S in VA.

27- DC power.

28- Inverter losses in VA.

29- Inverter output power factor.

30- Theta in radian.

31- Reactive power Q in Var.

After analyzing the data, it was noticed that no major or only very slight changes that occurred to the recorded data in one minute. Therefore, to optimize the analysis and the validation part of the model, data file for each day was averaged for 60 second period (1-minutes resolution). The file size changed from 54000 line to only 900 lines for 15 hours a day.

# CHAPTER 4

# RESULTS AND DISCUSSION

In this chapter validating the model using the collected data will be discussed. In addition, a proposed error function will be utilized to understand the factors that affect the system performance.

## 4.1 Validating Manufacture Model

In order to validate the model, the collected data will be used as an input to the constructed model. The data inputs to the model are:

1- Online irradiation value.
2- Online module temperature value.
3- The equivalent load resistor. This is found by dividing DC voltage by DC current at the central box.

Additional factor needs to be considered while validating the model is the cleaning day. The modules are cleaned one time monthly and takes between two to three days to be completed. This is due to the large area and the location of modules that are located on top of car parking roof. The cleaning job always start at night to maximize the power generation at noon time. Figures 22-32 demonstrate an example of model validation after the cleaning day and before the cleaning day.

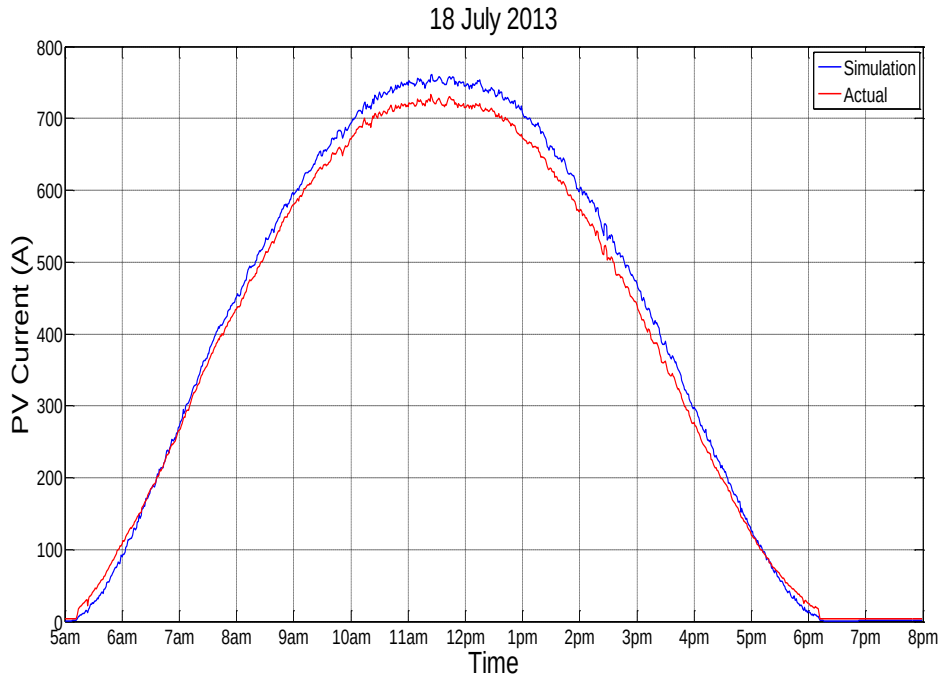


**Figure 22: Clean Day Current Curve**

Figures 22-24 shows in clean day the difference between the mathematical model and the online data for current, voltage and power respectively.

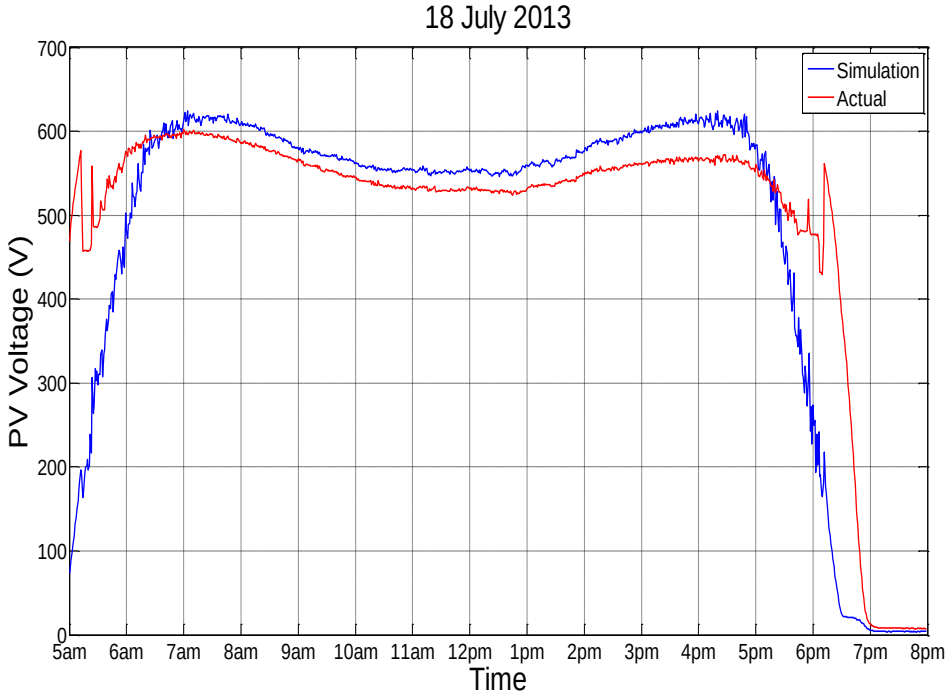


**Figure 23: Clean Day Voltage Curve**

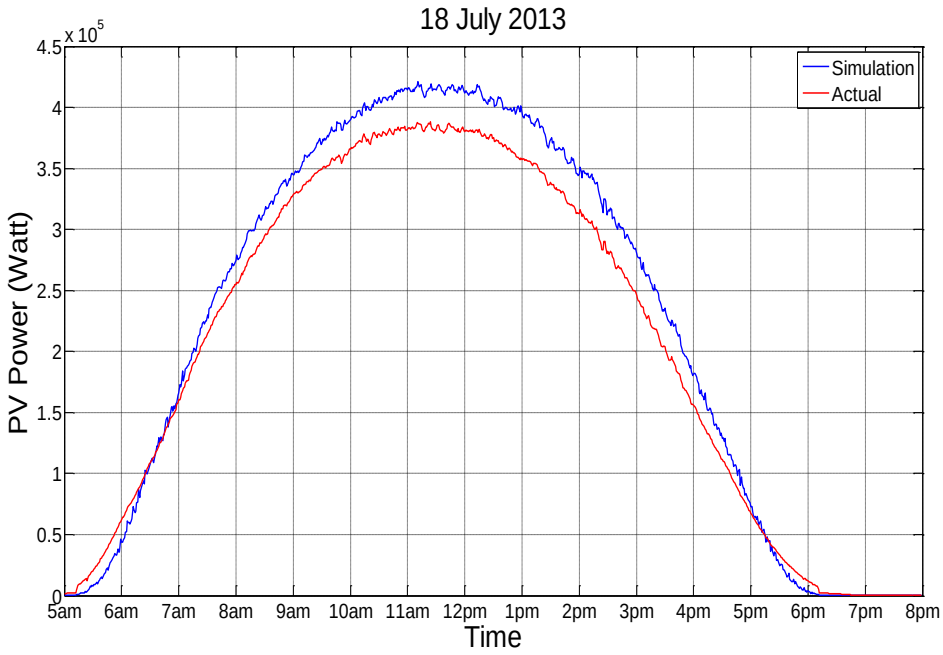


**Figure 24: Clean Day Power Curve**

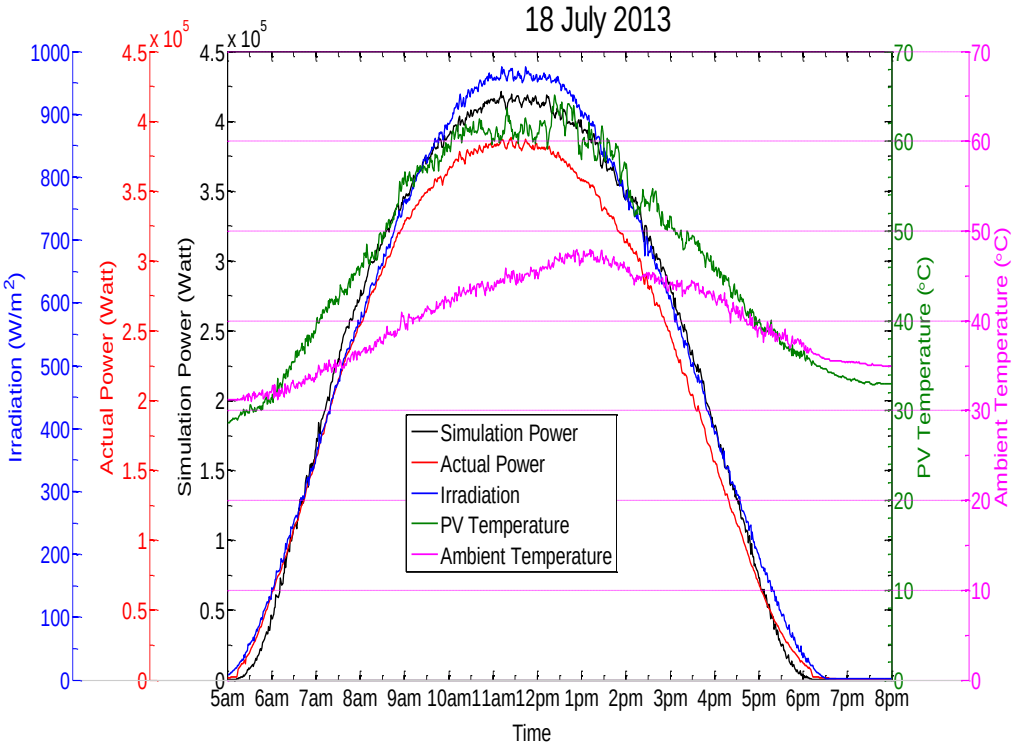


**Figure 25: Clean Day Performance Curve**

Figure 25 shows the clean day system power generation with variation in irradiation and temperature. However, even with smooth irradiation, the high temperature limits the total generation power to 50% of the rated power.

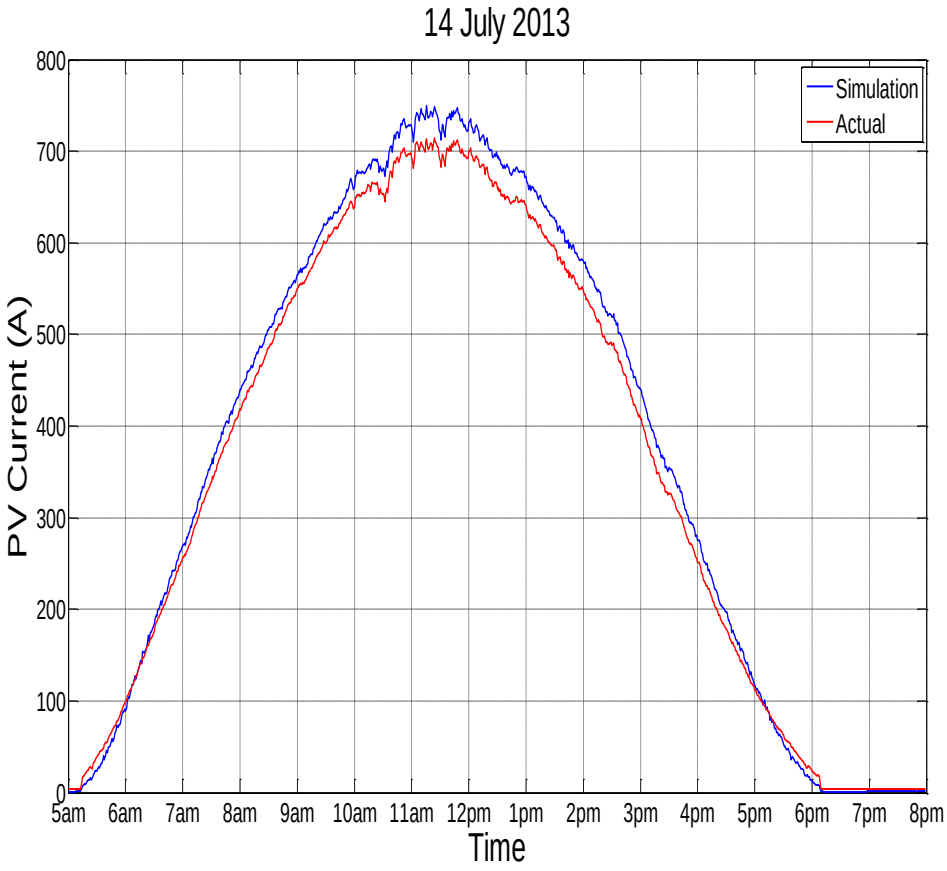


**Figure 26: Dusty Day Current Curve**

Figures 26-28 shows in dusty day the difference between the mathematical model and the online data for current, voltage and power respectively.

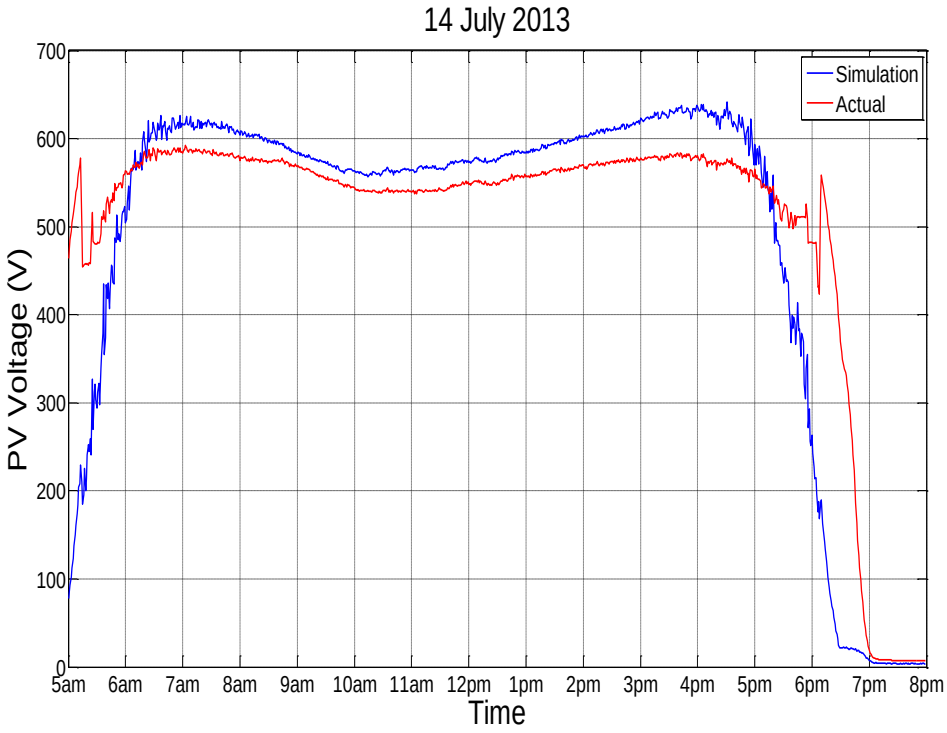


**Figure 27: Dusty Day Voltage Curve**

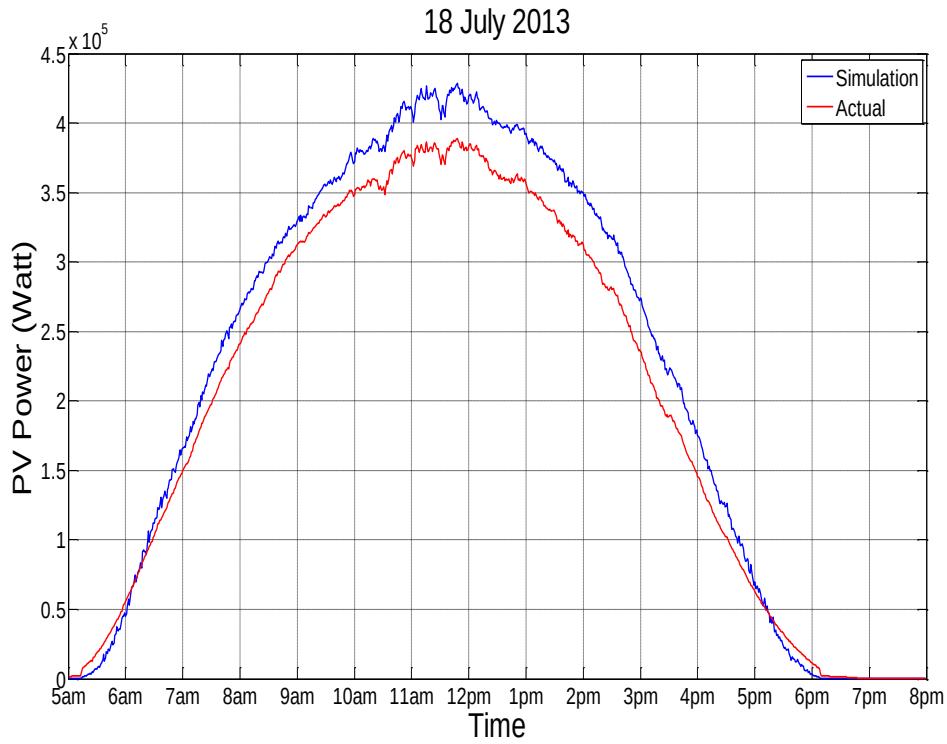


**Figure 28: Dusty Day Power Curve**

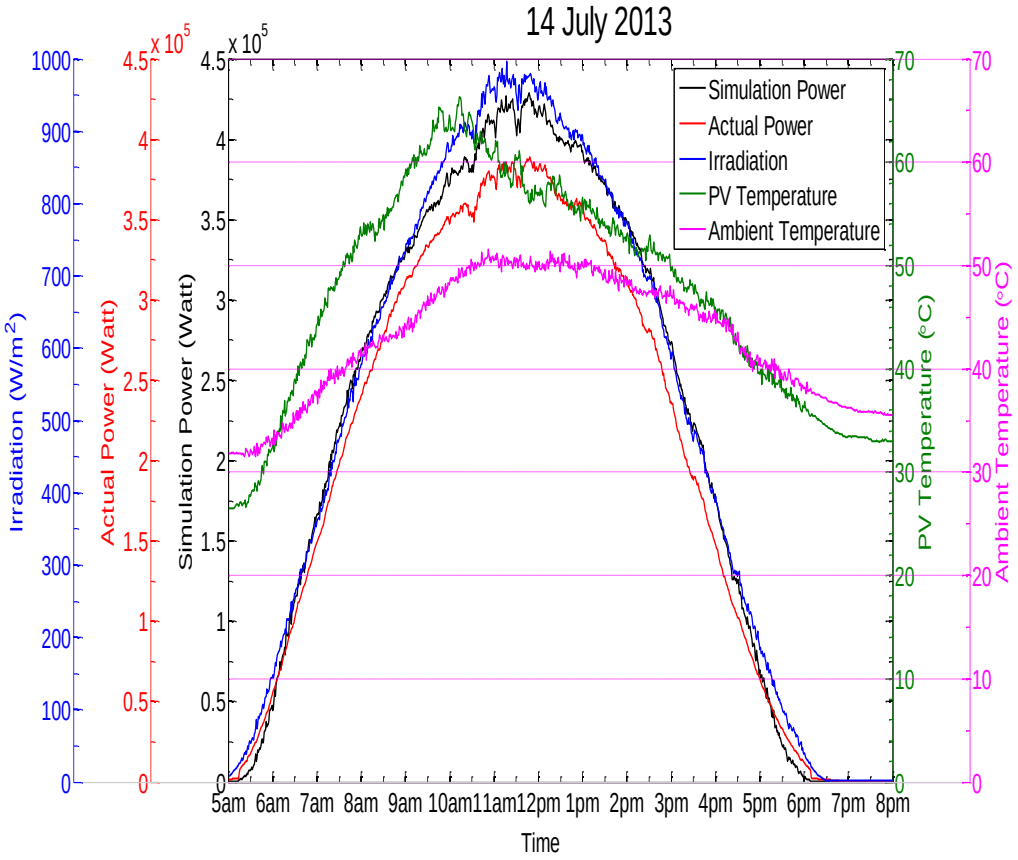


**Figure 29: Dusty Day Performance Curve**

Figure 29 shows the dusty day system power generation with variation in irradiation and temperature. However, even with smooth irradiation, the high temperature limits the total generation power to 50% of the design power.

In order to see the difference between clean and dusty panels, it is required to select similar sections in the system with exact number of PV panels. Reference to table 6, section 3 and section 5 both have 930 PV panels. However, the PV data sheet has a power tolerance of 7% and -5% and the irradiation received by PV panels are not the same for clean and dusty days which will limit the system analysis to the difference in Energy for both sections with different days.

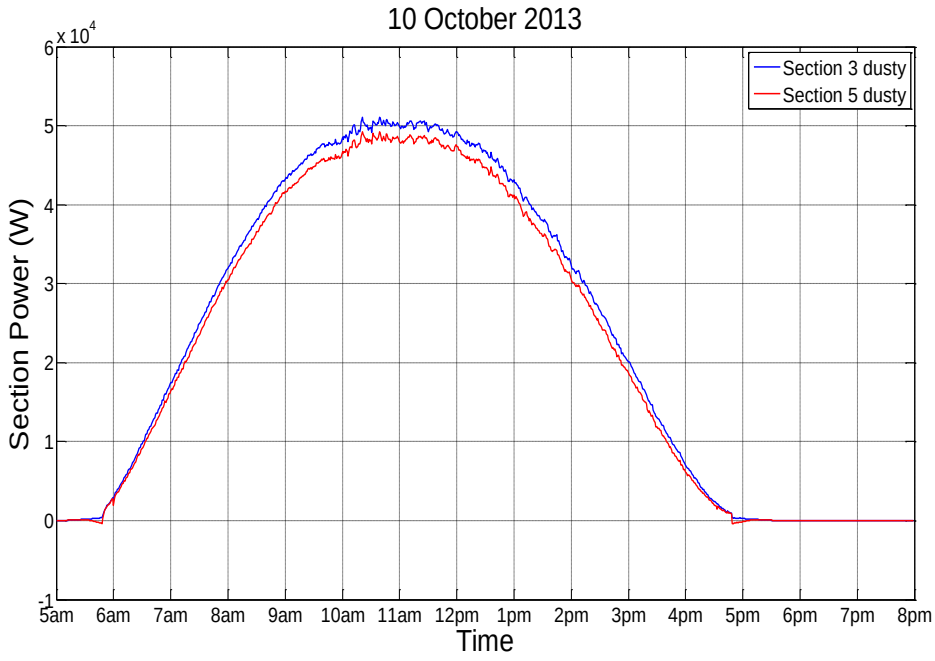


**Figure 30: Dusty Power Curves**

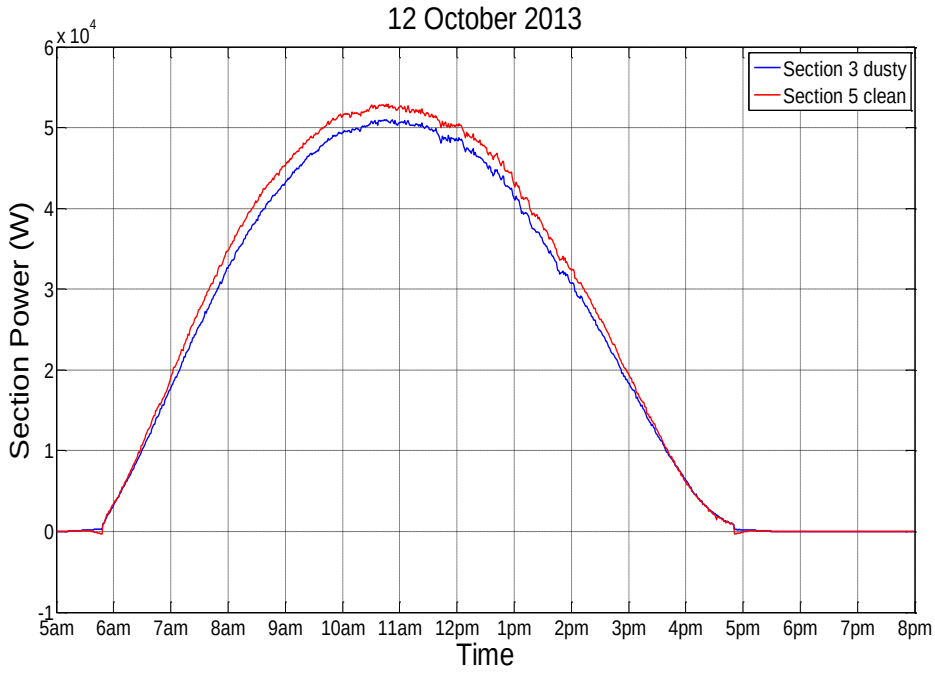


**Figure 31: Clean and Dusty Voltage Curve**

Figure 30 shows the power generation for sections 3 and 5 on dusty PV panels with difference in energy of 16.2 KWh. In figure 31, section 5 have been cleaned and gained

an energy difference of 31.98 KWh which gives an indication of approximate 9.7% increase of generated energy.

Investigating deeply on above figures provides the below results:

1- Both clean and dusty days provide good curve pattern with some error. In addition to the increase error margin in the case of dusty day.
2- Both clean and dusty days provide a clear non-linearity at the first and last hour of generation.
3- The result of both current and voltage are shown in the power curve. It was also clear that due to the high ambient temperature, the maximum power output reach to only 50% of rated maximum power. However, the power curve is smooth even the irradiation is fluctuating and both ambient and module temperature exceed 50°C.

Therefore, it is necessary to investigate the variation in the parallel module resistor as it affect the total current generation and hence the total performance. Next section will discuss the issue with parallel resistor.

# CHAPTER 5

# SYSTEM MODEL ENHANCEMENT

## 5.1 Parallel Module Resistor

In order to find the variation in parallel resistor, the voltage curve fitting between the online DC voltage and the model simulation is used. A loop function is used with voltage average error of 0.0001. The loop will adjust the $R_p$ value each point of simulation to match the voltage output as shown in figure 32. All other model parameters are kept without any change. It was noticed during the simulation that $R_p$ value could reach a very high value and hence, the maximum limit was set to 120 Ω.

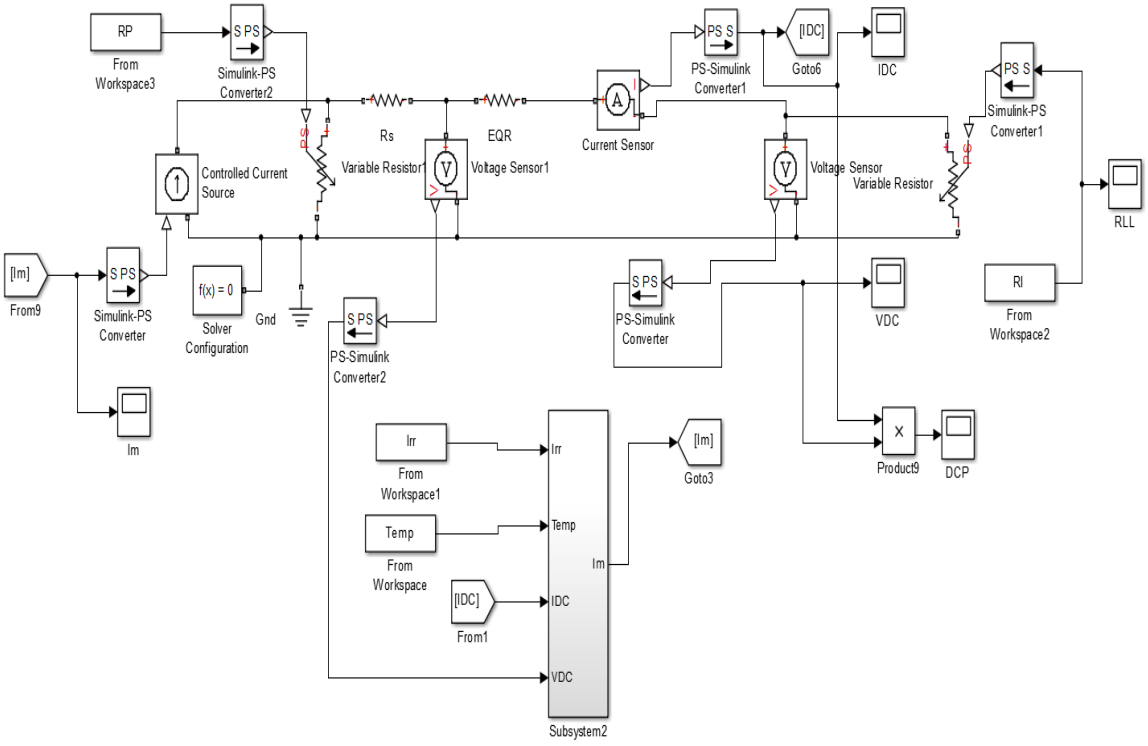


**Figure 32: Modified Model including variable Rp**

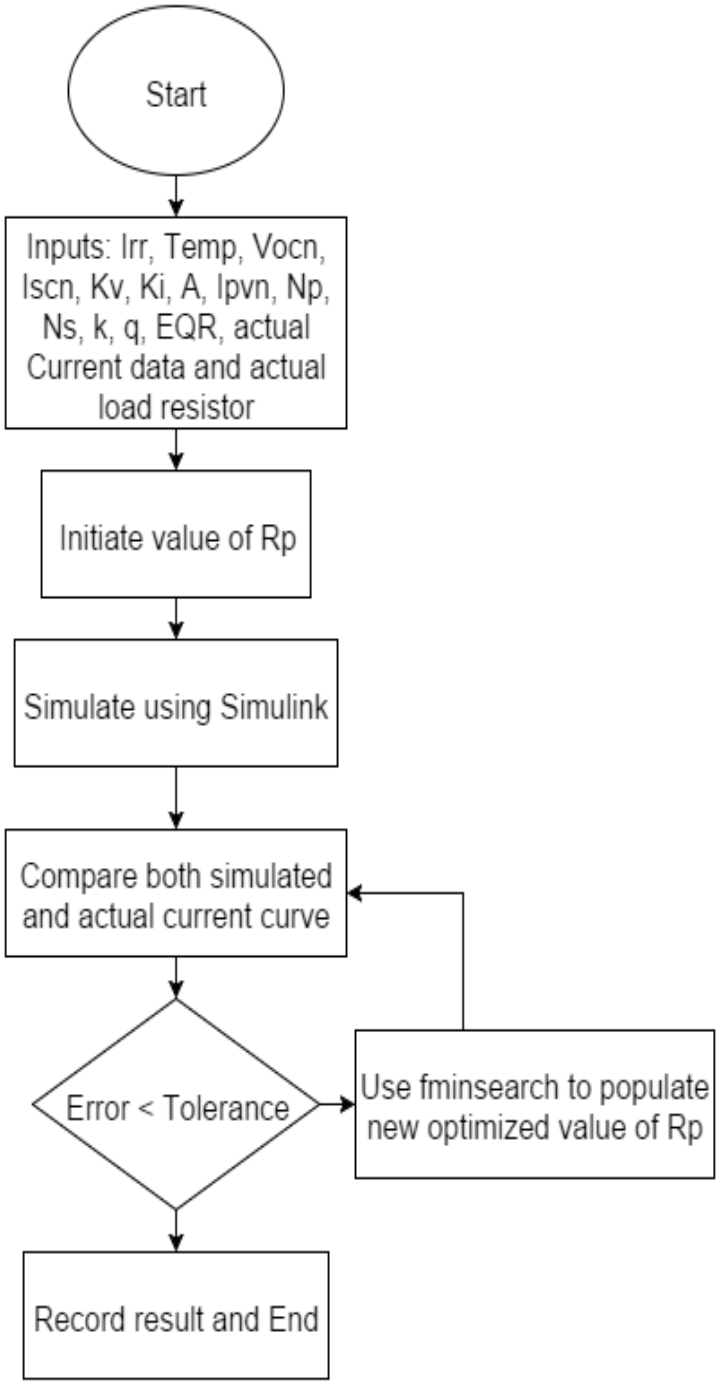


**Figure 33: Algorithm for variable Rp development**

The simplified flowchart of the iterative modeling algorithm is demonstrated in figure 33.

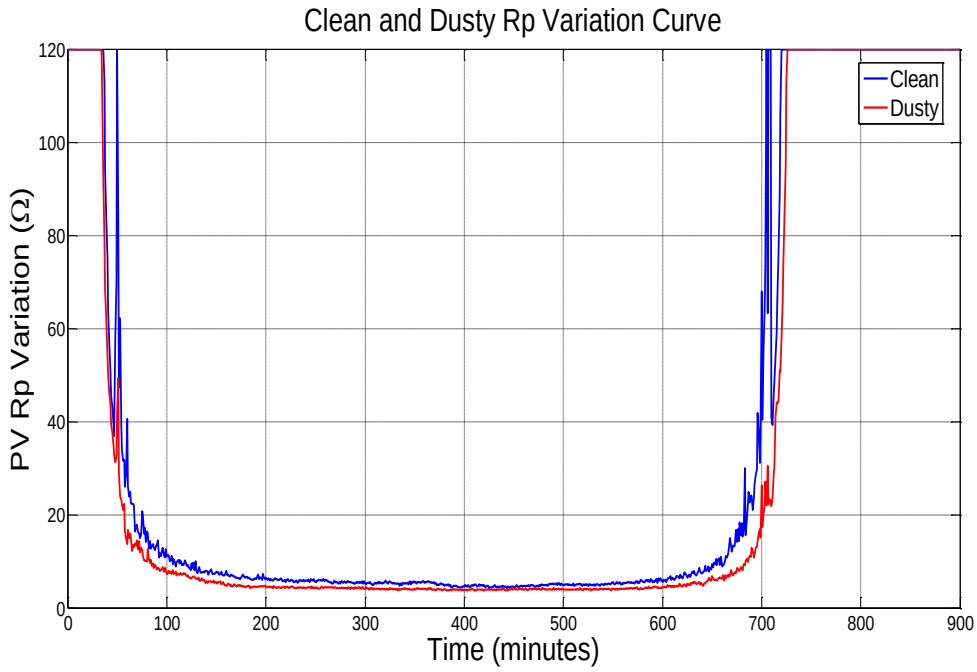


**Figure 34: Clean and Dusty Curve with Variable Rp**

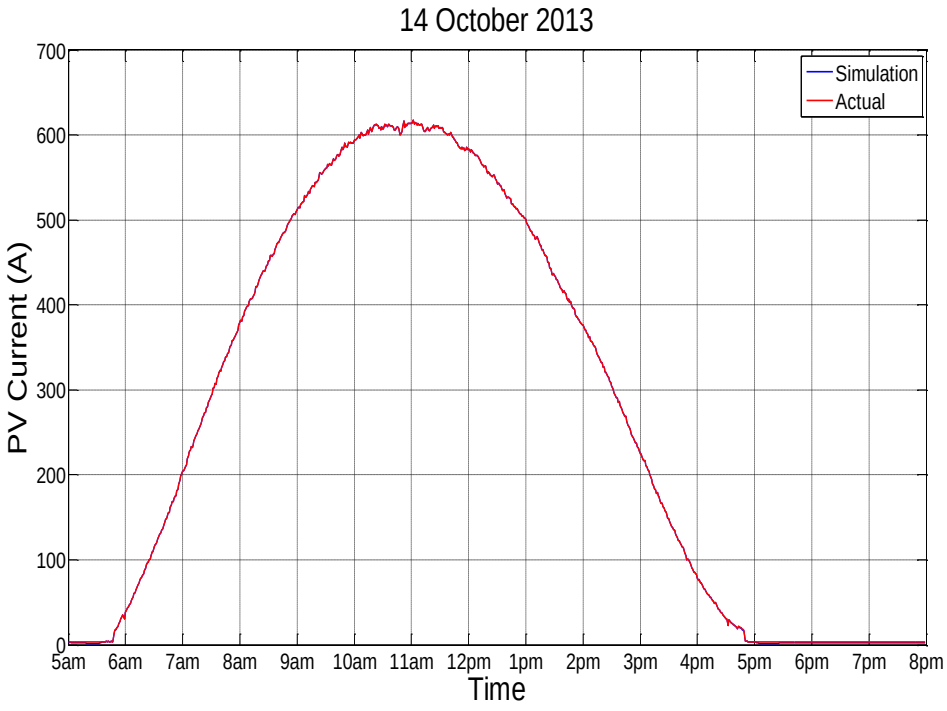


**Figure 35: Clean Day Current Curve with Variable Rp**

Figure 34 shows the $R_p$ variation for clean and dusty days. It is clear that the dusty days will have lower $R_p$ values as higher circulating current is occurring. Figure 35 shows that

the online and the simulation results are overlapped which validate the simulation result. However, figure 36 shows the non-linearity effect to the mathematical model for low irradiation values.

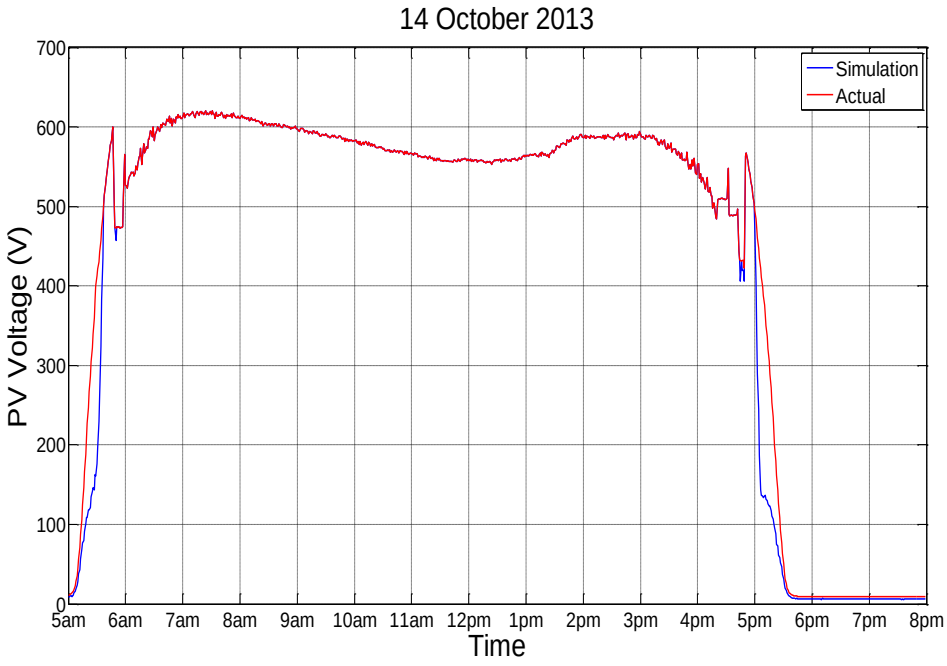


**Figure 36: Clean Day Voltage Curve with Variable Rp**

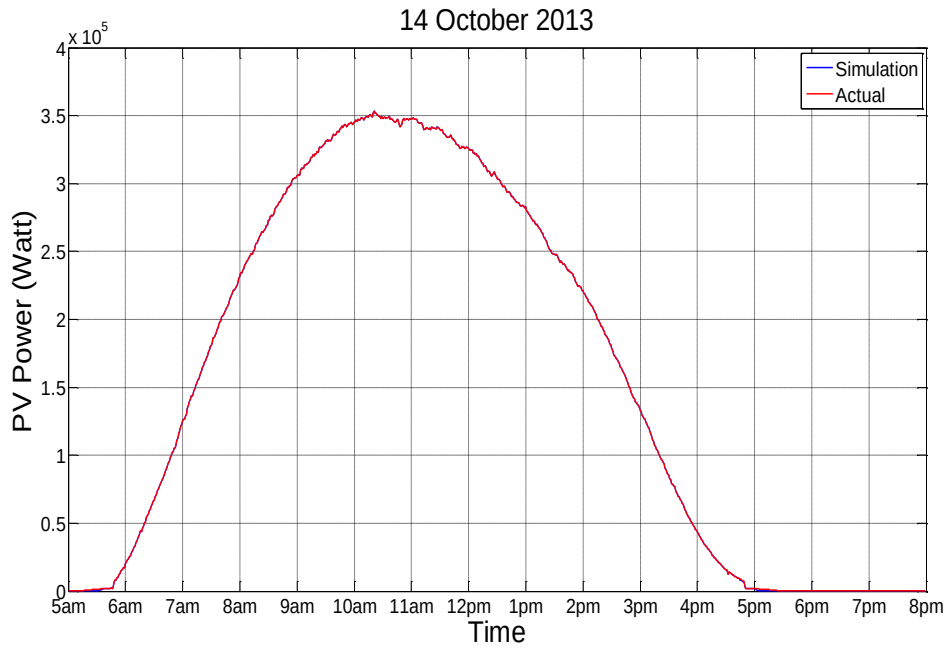


**Figure 37: Clean Day Power Curve with Variable Rp**

Even with the non-linearity issues, figure 37 demonstrate the overall power generation simulation result is overlapped with the online data.

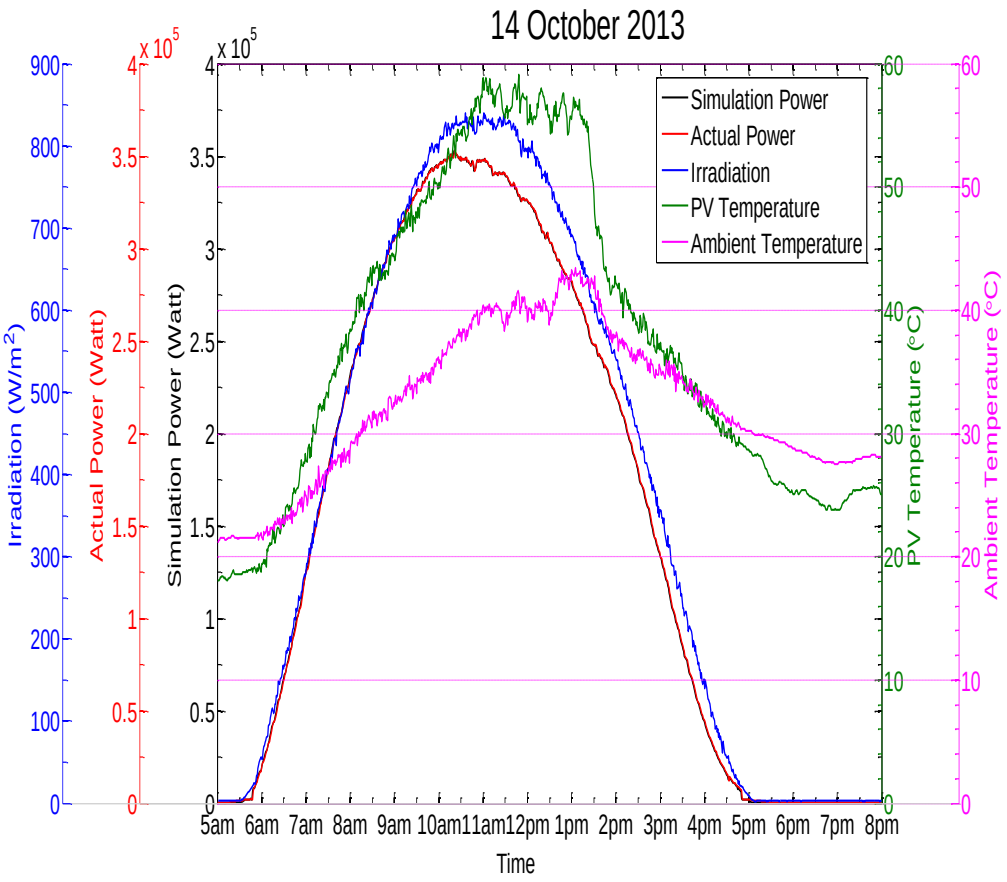


**Figure 38: Clean Day Performance Curve with Variable Rp**

Figure 38 shows that with variation in irradiation and temperature, the online and simulation results for the power generation is overlapped. Figure 39 shows that the online and the simulation results for current curve are overlapped and figure 40 shows the voltage curve with non-linearity effect at low irradiation.

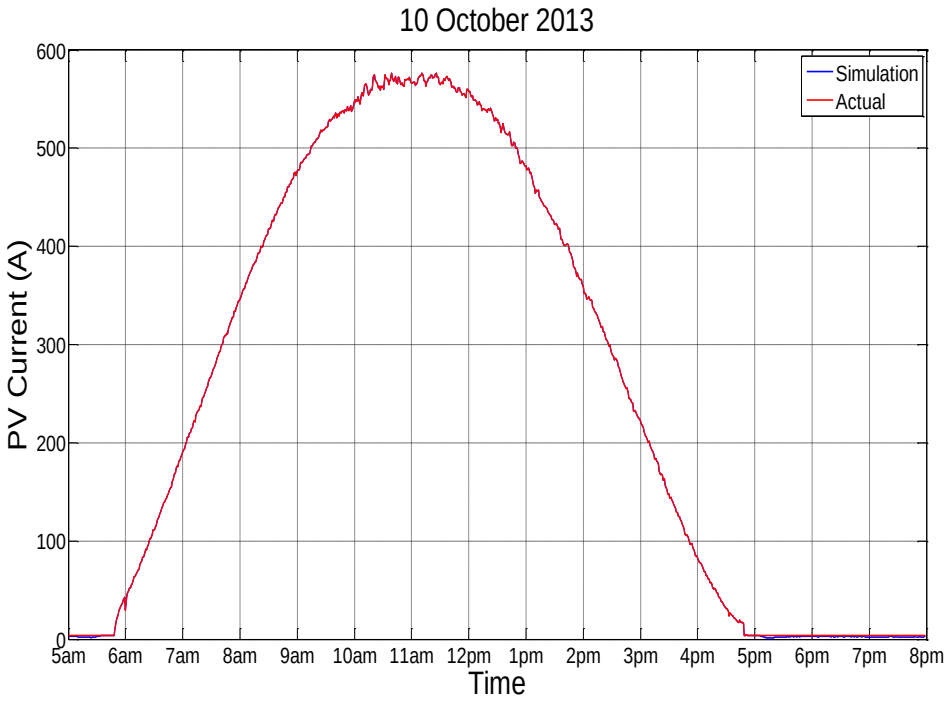


**Figure 39: Dusty Day Current Curve with Variable Rp**

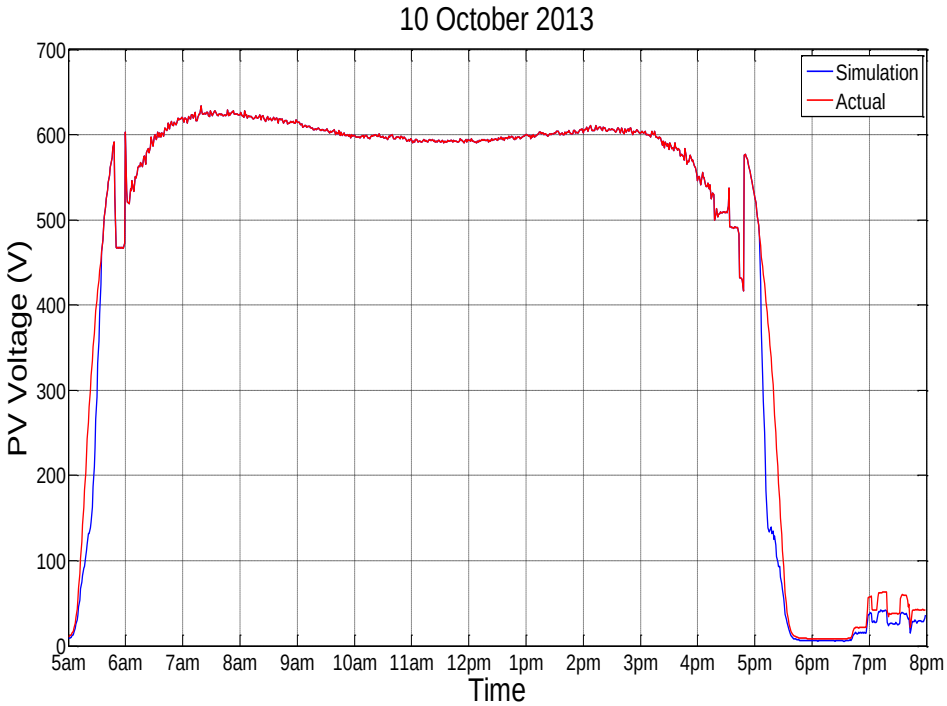


**Figure 40: Dusty Day Voltage Curve with Variable Rp**

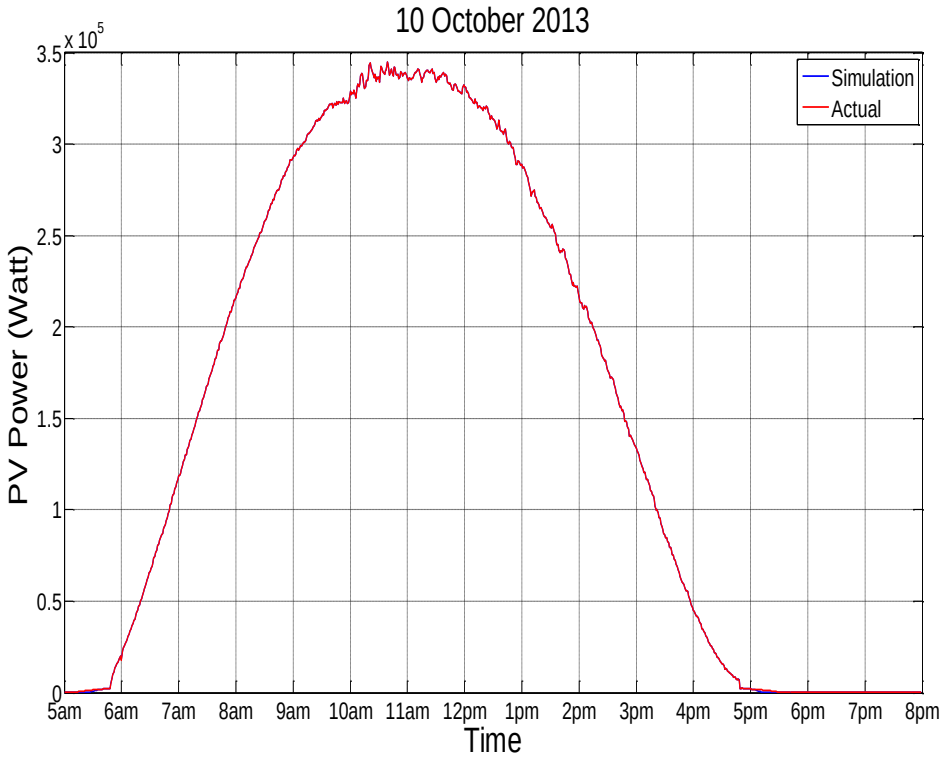


**Figure 41: Dusty Day Power Curve with Variable Rp**

Even with the non-linearity issues for dusty day, figure 41 demonstrate the overall power generation simulation result is overlapped with the online data. Figure 42 shows that with variation in irradiation and temperature for dust day, the online and simulation results for the power generation is overlapped.

It is clearly shown that the simulation results with variable $R_p$ provides an excellent fit to the online data. The following are the major findings:

1- The $R_p$ value for a dusty day is lower than the clean day. This clearly verify that the dust accumulation will increase the internal current circulation. Hence, the overall efficiency is reduced.

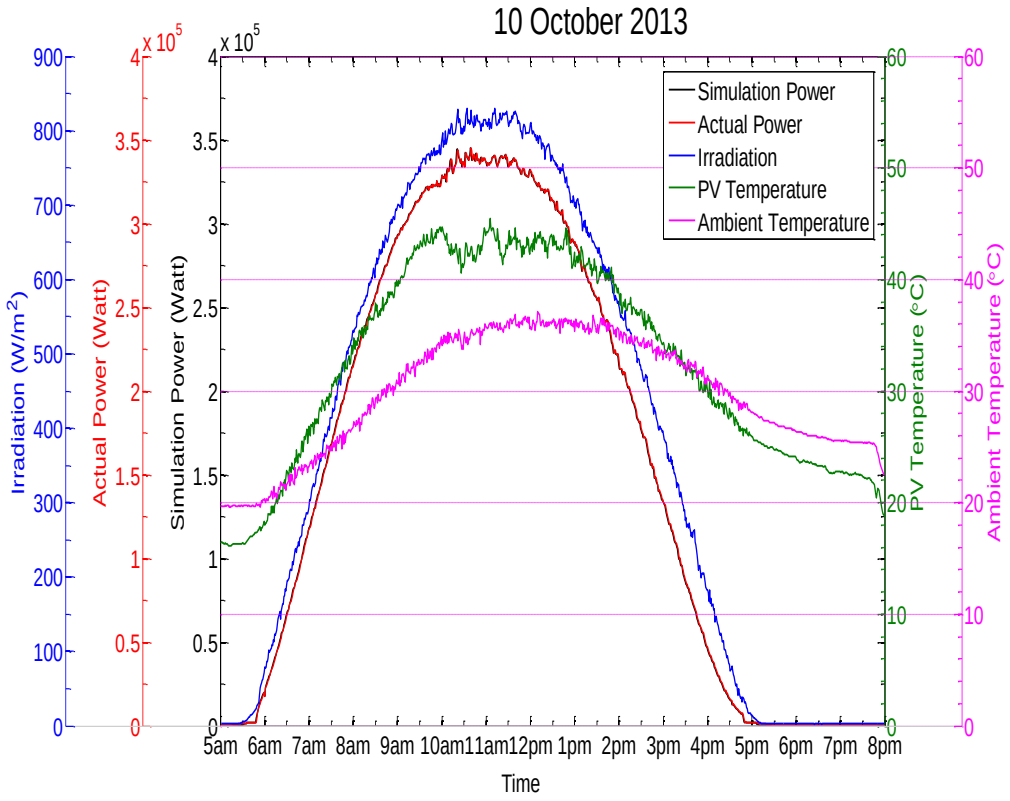


**Figure 42: Dusty Day Performance Curve with Variable Rp**

2- The voltage non-linearity is reduced by introducing the variable $R_p$.

3- An example of a clean day at noon time, the $R_p$ value is 5.722Ω. However, considering the series and parallel connections, the individual module $R_p$ value become 5.722*(423/15) = 161Ω equivalent to 54% of the identified module $R_p$ value of 298Ω.

With variable $R_p$ we can have an excellent simulation results, but what are the parameters that contribute in this variation. As revealed that one of the environmental factors (i.e. dust) will reduce $R_p$ value, it is logical to investigate more with environmental factors that will be explained in the next section.

## 5.2 Environmental Analysis

To achieve an optimum photovoltaic model, we need to find a relation between the variable parallel resistor and the environmental factors. These are:

1- Dust accumulation.

2- Wind speed

3- Humidity

4- Irradiation

5- Ambient temperature

### 5.2.1 Dust accumulation.

Dust factor will affect the $R_p$ value as explained in the previous sections. However, considering the size of the system and the non-availability of dust sensor, it is difficult to estimate the dust accumulation. Moreover, the dust could accumulate with different percentages at different locations. Also, as the system is designed with single voltage level, the voltage variation from each section/array will not be possible to track.

### 5.2.2 Wind Speed

Wind speed plays with two factors, module temperature and dust accumulation. High winds reduces the module temperature and when wind speed drops, it accumulate dust on photovoltaic surface. Hence, focusing on PV temperature and dust accumulation gain factor will consider the wind speed factor.

### 5.2.3 Humidity

Humidity is the amount of water vapor in the air. The increase in photovoltaic current is favored by low relative humidity. Low relative humidity, which means, low water vapor in the atmosphere gives rise to high solar flux. So the amount of irradiation received by the photovoltaic module will consider the humidity factor. Here, humidity could play a major role in Dhahran area as it will reduce the high irradiation during summer period. Based on the collected irradiation data for a full year, the irradiation reaches in summer (month of June 2013) to more than 1100 $W/m^2$.

### 5.2.4 Irradiation

Irradiation is the main source of energy to photovoltaic module but also is an environmental factor. During the year, different levels of irradiations are received by PV modules as the plant earth rotates around the sun and around itself. Moreover, clouds and humidity, as explained before, will change the irradiation levels received by PV modules. Also, more irradiation means more ambient temperature, hence more PV module temperature. It is clear that irradiation is directly related to the overall PV performance. Figures 43-44 show the relation between irradiation and variable parallel resistor.

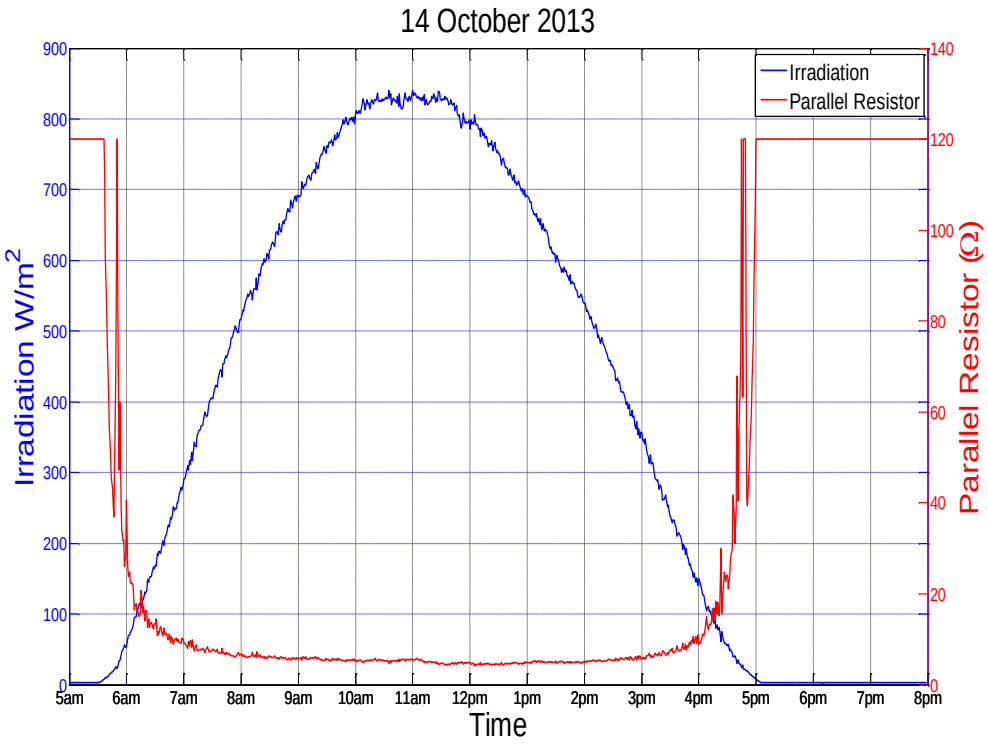


**Figure 43: Clean Day Irradiation Vs Parallel Resistor**

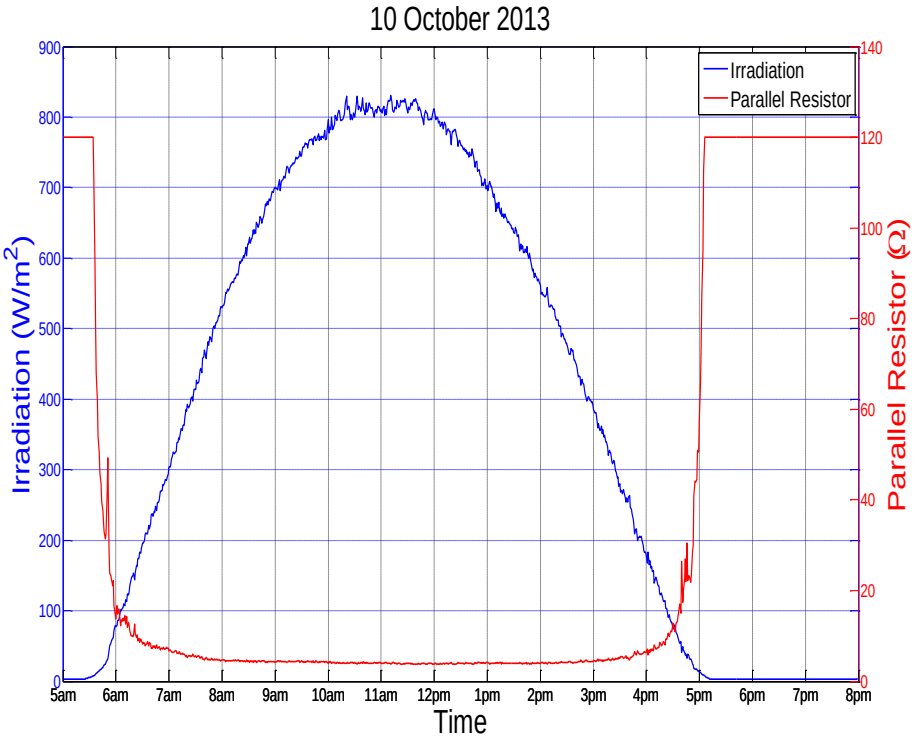


**Figure 44: Dusty Day Irradiation Vs Parallel Resistor**

### 5.2.5 Ambient temperature

This is one of the most important environmental factors that affect photovoltaic performance by affecting the PV module temperature. Reference to the earlier chapters, PV module temperature plays major role in total generated voltage. This means more temperature will cause more circulation current, hence less generated voltage. Moreover, high circulation currents reduces the expected life of PV module. Figures 45 and 46 show the relation between variable parallel resistor and the ambient and module temperatures.

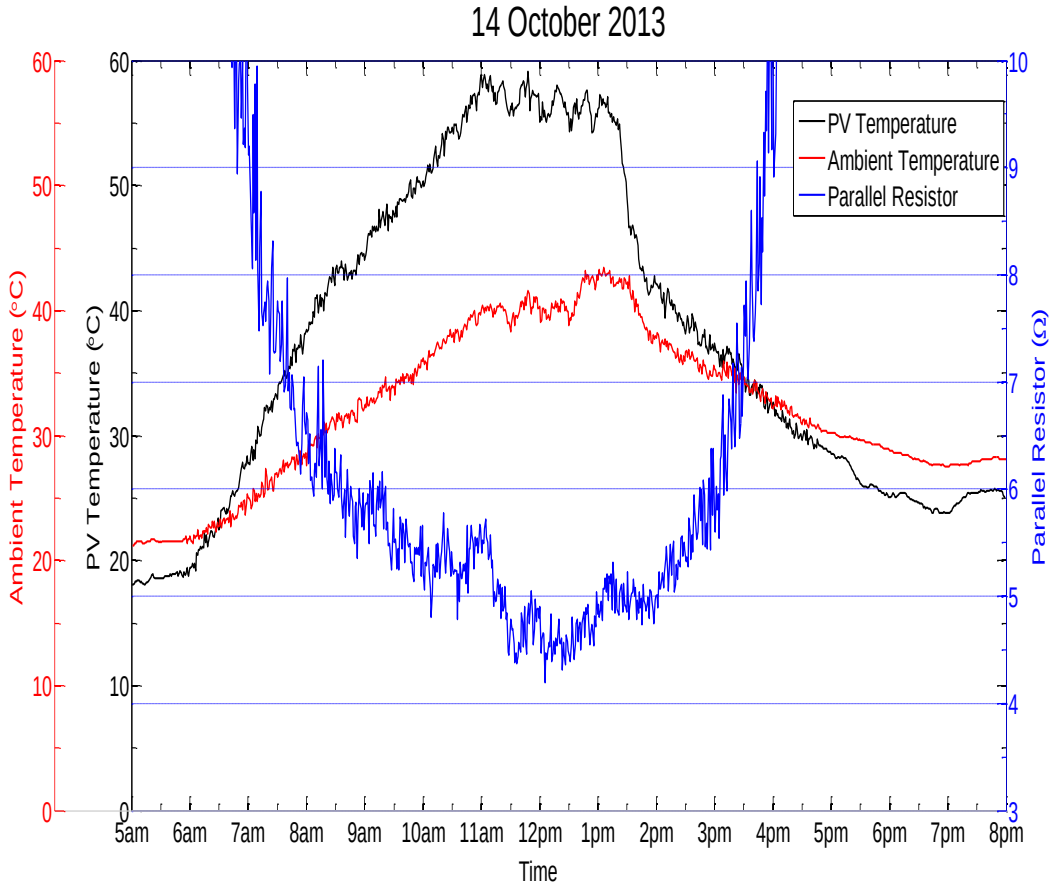


**Figure 45: Clean Day Temp. Vs Rp**

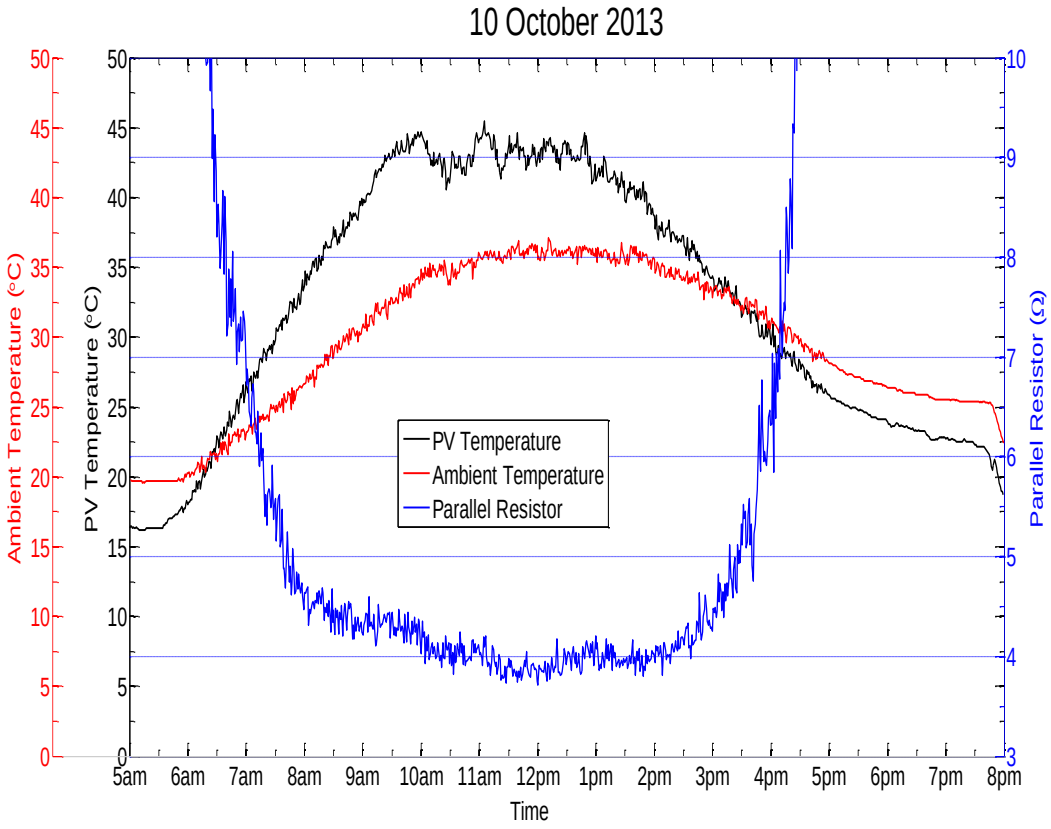


**Figure 46: Dusty Day Temp. Vs Rp**

As a summary of the environmental factors, the two main recorded environmental factors that affects the PV performance are irradiation and temperature. Considering the design model, both factors are integrated in photovoltaic generated current. However, parallel resistor is considered as an input value that has been found in the previous section. Figures 47 and 48 show irradiation, Temperature, Ambient and parallel resistor in one plot and figures 49 and 50 includes terminal voltage and equivalent load resistor.

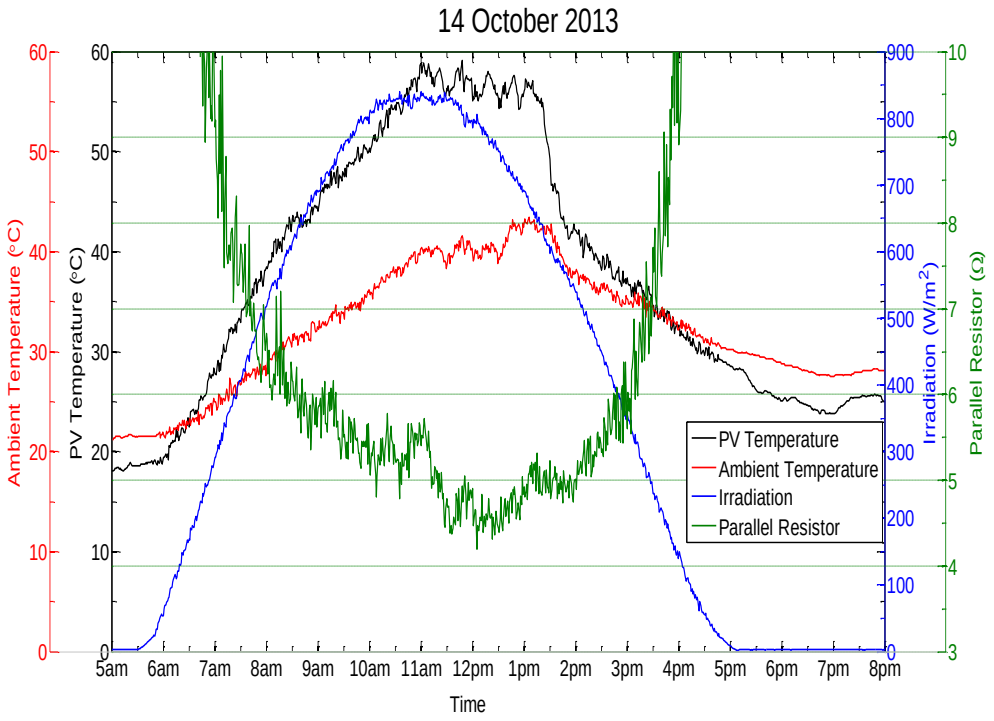


**Figure 47: Clean Day Irradiation, Temp., Ambient and Rp**

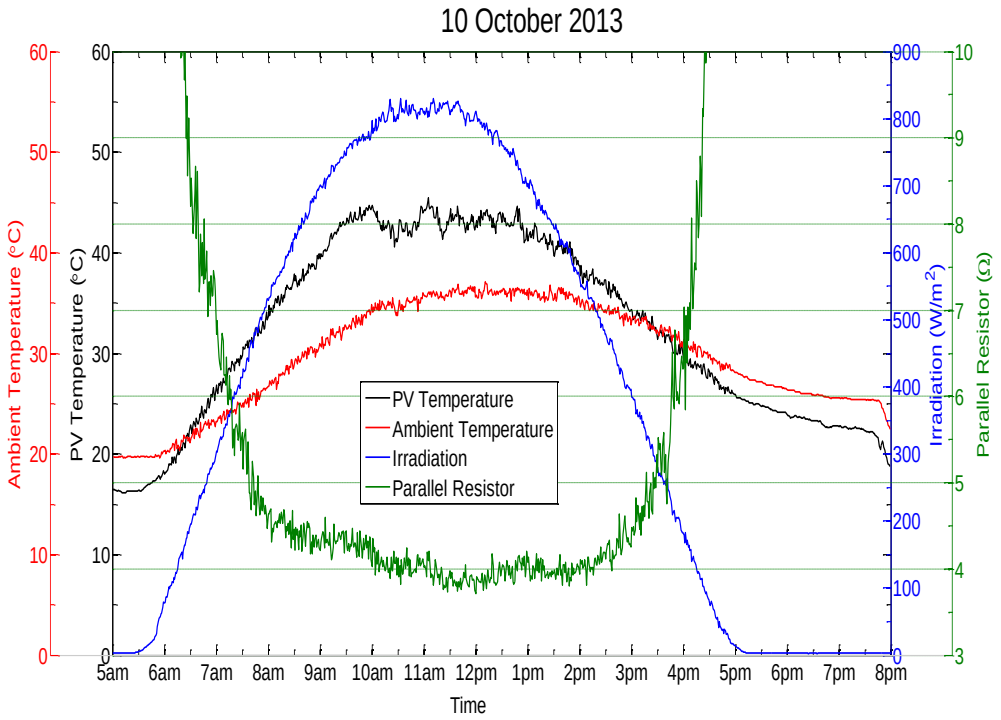


**Figure 48: Dusty Day Irradiation, Temp., Ambient and Rp**

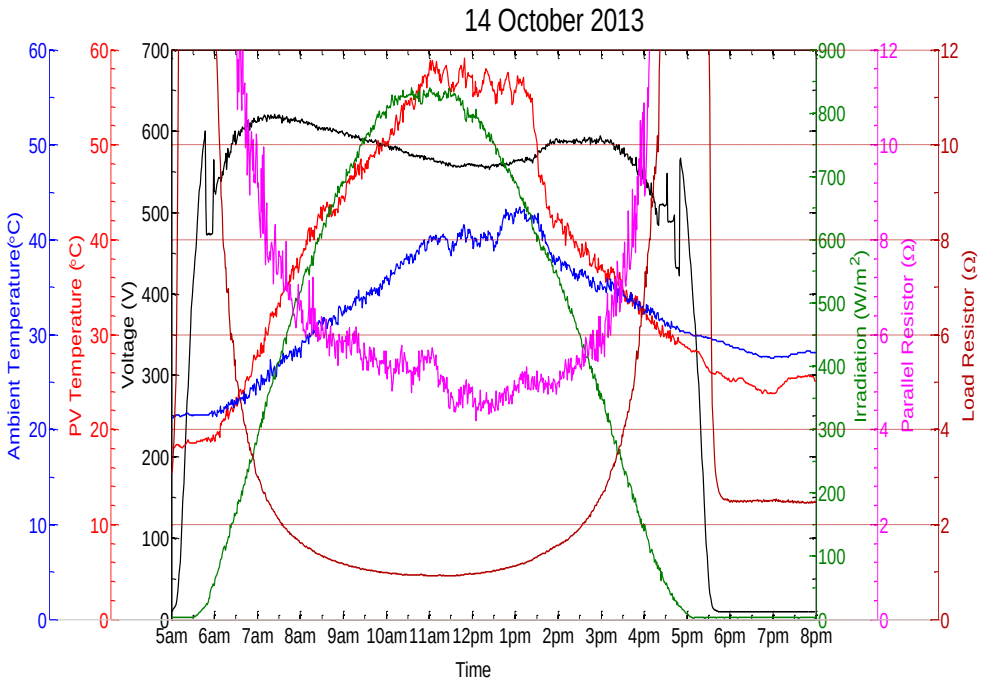


**Figure 49: Clean Day Performance with Rp**

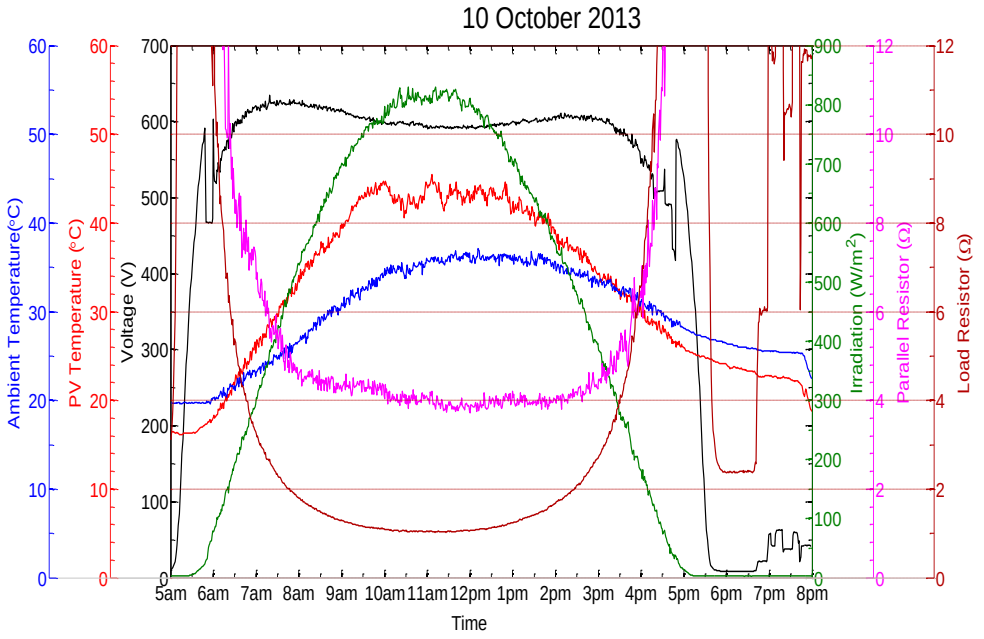


**Figure 50: Dusty Day Performance with Rp**

Using Matlab function (fminsearch) with different mathematical functions to include temperature and irradiation factors in forming the $R_p$ value provides clearer picture on parallel resistor variation. Equations 12-18 are the proposed mathematical functions used

to derive $R_p$. These functions were derived based on trial and error technique and hundreds of combination were used to find the best fit. These functions includes the effect of irradiation, temperature and the change in load resistor. The unknown parameters (X1, X2, X3, X4, X5, X6, X7, and X8) are to be found by the fminsearch function in every iteration. In each iteration, the simulation result with the online actual result of the generated current are compared. Then, based on the error value, the function will train itself to propose a new values of the unknown parameters. Once, the error target is achieved the simulation will end. Hence, the unknown parameters will be recorded.

$$F1 = X1 * R_{pn} * (\frac{Irr}{1000}) \quad (12)$$

$$F2 = R_{pn} * (\frac{Irr}{1000})^{X2} \quad (13)$$

$$F3 = X3 * R_{pn} * \left(\frac{Temp}{25}\right) * e^{2*X4(\frac{Temp}{25}-1)} \quad (14)$$

$$F4 = X5 * R_{pn} * \left(\frac{Irr}{1000}\right) * e^{X6(\frac{Irr}{1000}-1)} \quad (15)$$

$$F5 = \frac{X7}{R_{load}} \quad (16)$$

$$F6 = X8 \quad (17)$$

$$R_p = F1 + F2 + F3 + F4 + F5 + F6 \quad (18)$$

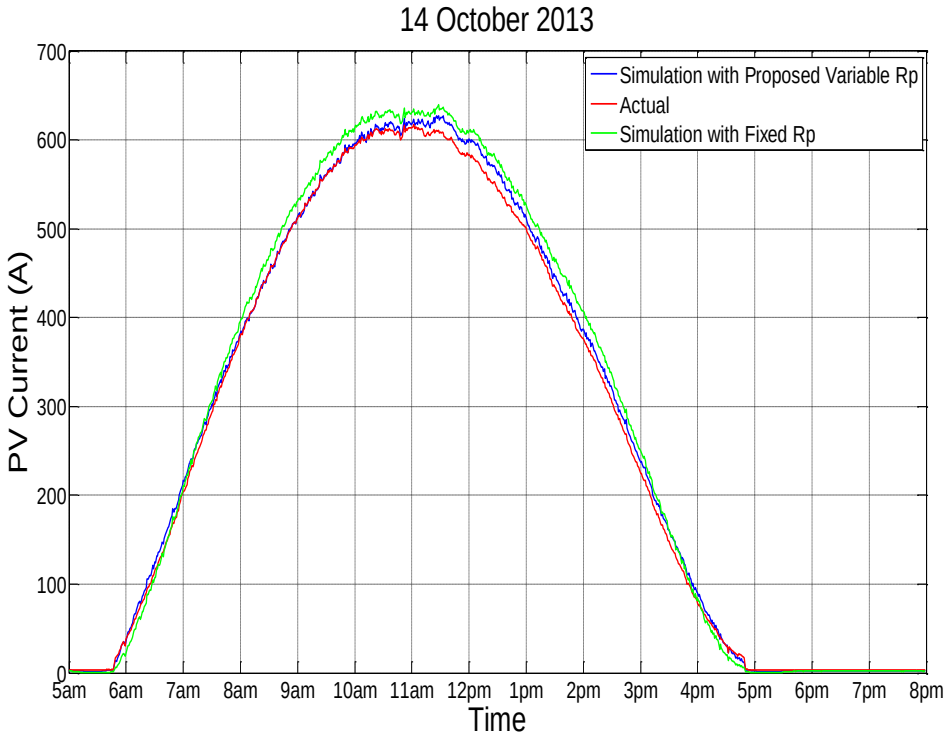


**Figure 51: Current Curve with Modified Rp**

Curve fitting technique with Matlab function (fminsearch) was used to find the values of X1 to X8 and the results of one day example are shown in figures 51-54. However, X1-X8 have different values for each selected day. Hence, to find an optimum values, a clean day with medium weather conditions that includes variation in irradiation and temperature was used. Figure 51 shows the result of current curve for fixed Rp, proposed variable Rp and the online collected data. The performance of the proposed parallel resistor is better than a fixed Rp value. Figure 52 shows the result of voltage curve were the average value of proposed Rp is better than the fixed one. However, it is clear that the non-linearity of the module performance affect mostly the generated voltage.

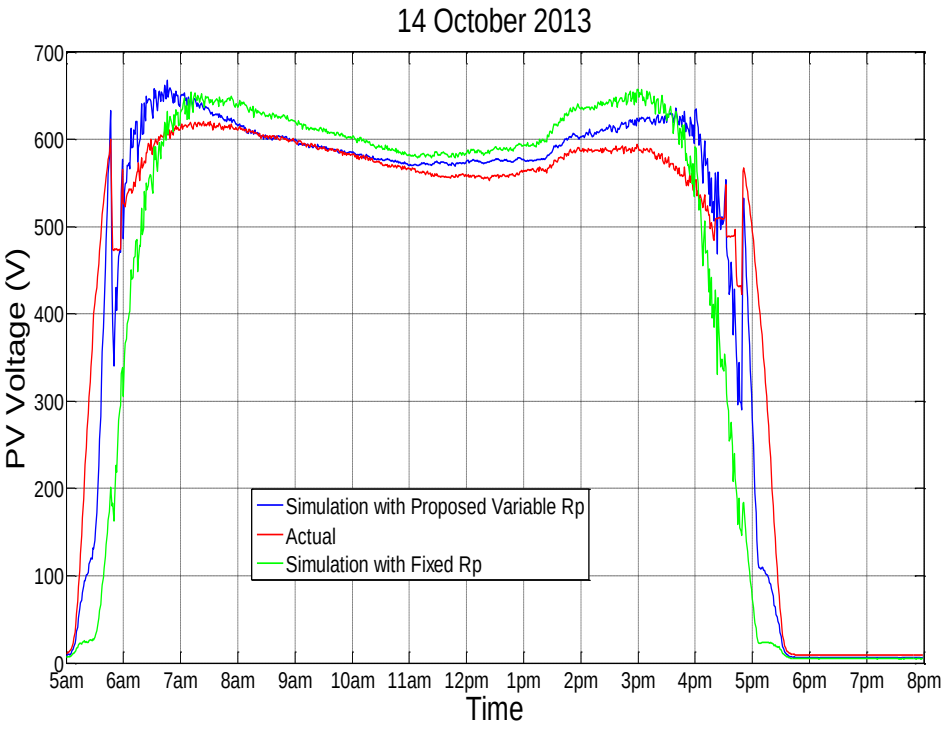


**Figure 52: Voltage Curve with Modified Rp**

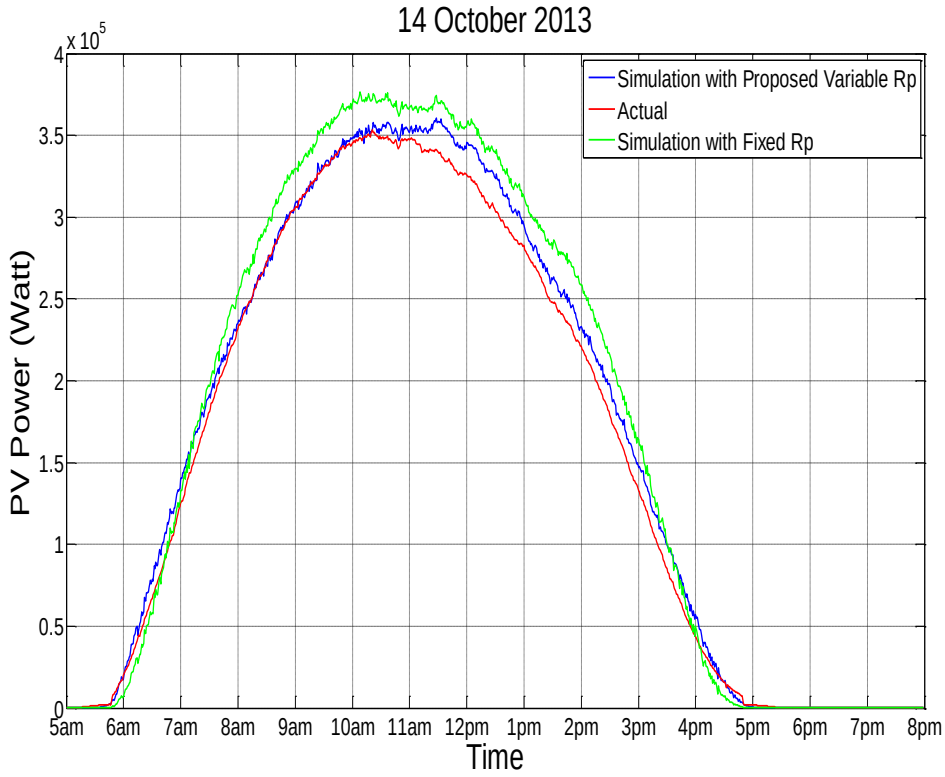


**Figure 53: Power Curve with Modified Rp**

Figure 53 shows the power result of the system. At the peak time, the proposed Rp provides a power result that is close to the online data but with fixed Rp, the difference is more than 15,000 watts. The values of X1 to X8 are:

X1= -3.80362

X2= -0.34459

X3= -2.40028

X4= -0.21909

X5= -0.24734

X6= 4.39340

X7= 36.83642

X8= 22.74202

The graphs shows that current and power provides an acceptable simulation results. However, the non-linearity region for the voltage needs more deep investigation. The proposed function of parallel resistor was used for different clean and dusty days with satisfactory results. Moreover, the proposed model can be used for future system designs and for forecasting the system generated power.

# CHAPTER 6

# CONCLUSION

Having all the analysis and the results found above, it is quite possible to conclude the below points:

- Parallel resistor used in modeling a photovoltaic system is not a fixed ohmic value. It was shown that with irradiation and temperature changes, the parallel resistor is changing too.
- With clean photovoltaic module, the parallel resistor change pattern will follow, with certain limitation, the irradiation change pattern. But with dusty modules, the parallel resistor change pattern is smoother than a clean day and doesn't follow the irradiation pattern.
- Changes in series resistor value is very small that can be neglected during the simulation.
- There is a voltage non-linearity when the irradiation value is below 300 $W/m^2$. Also, the parallel resistor reached high value.
- Based on the collected data for one year with all-weather seasons, the PV technology used in this work have withstand the high temperature in Dhahran area. However, with high irradiation and high temperature the generation performance is reduced rapidly.
- The enhancement to the solar mathematical model with a function for the parallel resistor shows a better results than the normal model. This achievement can be

used for forecasting the system power generation for industrial and financial purposes. Also, it can be used to enhance future solar system designs.

## 6.1 Future Work

The work done here can be improved by following these recommendations:

- The proposed design can be applied for larger system.
- The non-linearity region for photovoltaic generated power at low irradiation can be investigated.
- Investigate the relation between temperature, irradiation and parallel resistor in more details.
- Investigate the relation between temperature, irradiation and diode ideal factor.
- Investigate the relation between temperature, irradiation and short circuit current coefficient.
- Investigate the relation between temperature, irradiation and open voltage coefficient.

# APPENDIX

**Supplier** Solar Frontier K.K.
**Type** SF80-EX-B
Aktuell ☐

Record-nr.: 24511

**Standard data**

| | |
|---|---|
| Nominal power | 80 W |
| Power tolerance pos | 7 % |
| Power tolerance neg | -5 % |
| Origin | |
| BIPV ☐ | |
| Module efficiency | 10,11 % |
| Cell manufacturer | |
| Cell type | CIS |
| Cell shape | |
| Cell efficiency | % |
| Cells per module | |
| Guarantee of power 1 | years |
| Guarantee of power 1 | % of Pnom |
| Guarantee of power 2 | years |
| Guarantee of power 2 | % of Pnom |
| Product guarantee | years |
| Distribution area | |
| Internet | www.solar-frontier.com |
| Produced from | |
| Produced until | |

**Picture**

No picture available

Approvals
CE
IEC 61646
IEC 61730
Safety class II

Remarks

**Mechanical data**

| | |
|---|---|
| Length | 1235 mm |
| Width | 641 mm |
| BIPV: Visible length a. inst. | mm |
| BIPV: Visible width a. inst. | mm |
| Thickness frame | 35 mm |
| Thickness box | 35 mm |
| Frame type | |
| Composition | |
| Junction box / Cable junction box | |
| Connection | MC4 |
| Weight | 12,4 kg |

**Electrical data**

| | | Vmpp | | Impp |
|---|---|---|---|---|
| Voc at 1000 W / m² | 56,5 V | 1000 W / m² | 41 V | 1,95 A |
| Isc at 1000 W / m² | 2,26 A | 950 W / m² | V | A |
| Voc at -10°C and 1000 W / m² | 62,23 V | 900 W / m² | V | A |
| Vmpp at 70°C and 1000 W / m² | 35,65 V | 850 W / m² | V | A |
| Coefficient of voltage | -0,29 %/°C | 800 W / m² | 38,7 V | 1,52 A |
| Coefficient of current | 0,03 %/°C | 750 W / m² | V | A |
| Coefficient of power | -0,35 %/°C | 700 W / m² | V | A |
| NOCT at 800 W / m² | 47 °C | 650 W / m² | V | A |
| Max system voltage EU | 1000 V | 600 W / m² | V | A |
| Max system voltage US | V | 550 W / m² | V | A |
| Serial resistance | ohms | 500 W / m² | V | A |
| Isolation resistance | ohms | 450 W / m² | V | A |
| | | 400 W / m² | V | A |
| | | 350 W / m² | V | A |

# NOMENCLATURE

| | |
|---|---|
| $I_{ph}$ | Photovoltaic generated current |
| $I_{phn}$ | Photovoltaic nominal generated current |
| $I_s$ | Diode saturation current |
| $I_{sn}$ | Diode nominal saturation current |
| $I_{sc}$ | Photovoltaic short circuit current |
| $V_{oc}$ | Photovoltaic open circuit voltage |
| G | Irradiation in $W/m^2$ |
| $G_n$ | Nominal Irradiation in $W/m^2$ |
| K | Boltzmann Constant |
| T | Temperature |
| q | Electron electric charge, $q=1.6*10^{-19}$ C |
| DC | Direct Current |
| AC | Alternate Current |
| V | Voltage |
| I | Current |

| | |
|---|---|
| P | Power |
| PV | Photovoltaic |
| W | Watt |
| KW | Kilo Watt |
| A | Amper |
| m | Meter |
| Q | Reactive power |
| S | Apperant power (VA) |
| R | Resistance |
| $A_1$ | Ideal factor for the first diode |
| $A_2$ | Ideal factor for the second diode |
| $R_s$ | Series cell resistance |
| $R_p$ | Parallel cell resistance |
| $R_{pn}$ | Nominal Parallel resistance |
| Eg | The solar cell activation energy |
| $V_t$ | Thermal voltage |
| $k_1$ | Temperature exponent for first diode |

$K_I$ Short circuit current coefficient

$K_V$ Open circuit voltage coefficient

$N_s$ Series cells

$N_p$ Parallel cells

GB Giga Bytes

Ω Ohm

$X_1$ Constant 1

$X_2$ Constant 2

$X_3$ Constant 3

$X_4$ Constant 4

$X_5$ Constant 5

$X_6$ Constant 6

$X_7$ Constant 7

$X_8$ Constant 8

# References


[1] Eveloy, V., Rodgers, P. and Bojanampati, S., "Enhancement of Photovoltaic Solar Module Performance for Power Generation in the Middle East" 2012 28th Annual IEEE Semiconductor Thermal Measurement and Management Symposium (SEMI-THERM), pp. 87-98. DOI: 10.1109/STHERM.2012.6188831.

[2] Farhana, Z., Irwan, Y. M., Azimmi, R. M. N., Razliana, A. R. N. and Gomesh, N., "Experimental Investigation of Photovoltaic Modules Cooling System" 2012 IEEE Symposium on Computers & Informatics (ISCI), pp. 165-169. DOI: 10.1109/ISCI.2012.6222687.

[3] Mahmoud, S. A. and Mohamed, H. N., "Novel Modeling Approach For Photovoltaic Arrays" 2012 IEEE 55th International Midwest Symposium on Circuit and Systems (MWSCAS), pp. 790-793. DOI: 10.1109/MWSCAS.2012.6292139.

[4] Dhass, A. D., Natarajan, E. and Ponnusamy, L., "Influence of Shunt Resistance on the Performance of Solar Photovoltaic Cell" 2012 International Conference on Emerging Trends in Electrical Engineering and Energy Management (ICETEEEM), pp. 382-386. DOI: 10.1109/ICETEEEM.2012.6494522.

[5] Ali, Mir Shahid, Photovoltaic System Modeling and Analysis, December 2010.

[6] Surya Kumari, J. and Sai Babu, Ch., "Mathematical Modeling and Simulation of Photovoltaic Cell using Matlab-Simulink Environment" International Journal of Electrical and Computer Engineering (IJECE), Vol. 2, no. 1, pp. 26-34, 2012.

[7] Villalva, M. G., Gazoli, J. R. and Filho, E. R., "Comprehensive Approach to Modeling and Simulation of Photovoltaic Arrays" IEEE Transactions on Power Electronics, Vol. 24, No. 5 pp.1198-1208, 2009. IDO: 10.1109/TPEL.2009.2013862

[8] Tutorial: Electronic Circuits-Diodes/Transistors/FETs, Renesas Engineer School October 01 2013, http://am.renesas.com/edge_ol/engineer/02/index.jsp

[9] Izadian, A., Pourtaherian, A. and Motahari, S., “Basic Model and Governing Equation of Solar Cells used in Power and Control Applications” 2012 IEEE Energy Conversion Congress and Exposition (ECCE), pp. 1483-1488. DOI: 10.1109/ECCE.2012.6342639.

[10] Bhuvaneswari, G. and Annamalai, R., “Development of A Solar Cell Model in Matlab for PV Based Generation System” 2011 Annual IEEE India Conference (INDICON), pp. 1-5. DOI: 10.1109/INDCON.2011.6139509.

[11] Gow, J. A. and Manning, C. D., “Development of a photovoltaic array model for use in power-electronics simulation studies” IEE Proceeding - Electric Power Applications, Vol. 146, No. 2, pp. 193-200, 1999.DOI: 10.1049/ip-epa:19990116.

[12] Romero-Cadaval, E., Spagnuolo, G., Garcia Franquelo, L., Ramos-Paja, C. A., Suntio, T. and Xiao, W. M., “Grid-Connected Photovoltaic Generation Plants” IEEE Industrial Electronics Magazine, Vol. 7, No. 3, pp. 1-6, 2013. DOI: 10.1109/MIE.2013.2264540.

[13] Mahmoud, Y. A., Xiao, W. and Zeineldin, H. H., “A Parameterization Approach for Enhancing PV Model Accuracy” IEEE Transactions on Industrial Electronics, Vol. 60, No. 12, pp. 5708-5716, 2013. DOI: 10.1109/TIE.2012.2230606.

[14] Hejri, M., Mokhtari, H., Azizian, M. R., Ghandhari, M. and Soder, L., “On the Parameter Extraction of a Five Parameter Double-Diode Model of Photovoltaic Cells and Modules” IEEE Journal of Photovoltaics, Vol. 4, No. 3, pp. 915-923, 2014. DOI: 10.1109/JPHOTOV.2014.2307161.

[15] Babu, B. C. and Gurjar, S., “A Novel Simplified Two-Diode Model of Photovoltaic (PV) Module” IEEE Journal of Photovoltaics, Vol. 4, No. 4, pp. 1156-1161, 2014. DOI: 10.1109/JPHOTOV.2014.2316371.

[16] Rahman, S. A., Varma, R. K. and Vanderheide, T., “Generalised model of a photovoltaic panel” IET Renewable Power Generation, Vol. 8, No. 3, pp. 217-229, 2014. DOI: 10.1049/ite-rpg.2013.0094.

[17] Elkholy, A., Fahmy, F.H. and Elela, A.A., “A New Technique for Photovoltaic Module Performance Mathematical Model” 2010 International Conference on Chemistry and Chemical Engineering (ICCCE 2010), pp. 6-10. DOI: 10.1109/ICCCENG.2010.5560349.

[18] Xinqiang Xu, Mayers, M.M., Sammakia, B.G. and Murray, B.T., "Thermal Modeling of Hybrid Concentrating PV/T Collectors with Tree-shaped Channel Networks Cooling System" 2012 13th IEEE Intersociety Conference on Thermal and Thermomechanical Phenomena in Electronic Systems (ITHERM), pp. 1131-1138, DOI: 10.1109/ITHERM.2012.6231550.

[19] Farahat, M. A., "Improvement the Thermal Electric Performance of A Photovoltaic Cells by Cooling and Concentration Techniques" UPEC 2004 39th International Universities Power Engineering Conference, Vol. 1, pp. 623-628.

[20] Villalva, M. G., Gazoli, J. R. and Filho, E. R., "Modeling and Circuit-Based Simulation of Photovoltaic Arrays" 2009 Brazilian Power Electronics Conference, pp. 1244-1254. DOI: 10.1109/COBEP.2009.5347680.

[21] Sheik Mohammed, S., "Modeling and Simulation of Photovoltaic module using MATLAB/Simulink" International Journal of Chemical and Environmental Engineering, Vol. 2, No. 5 (2011), pp. 350-355.

[22] Ramaprabha, R., Mathur, B. L. and Sharanya, M., "Solar Array Modeling and Simulation of MPPT using Neural Network" 2009 Proceeding of International Conference on Control, Automation, Communication and Energy Conservation (INCACEC), pp. 1-5.

[23] Devaraj, D., Sakthivel, S. and Punitha, K., "Modeling of Photovoltaic Array and Simulation of Adaptive Hysteresis Current Controlled Inverter for Solar Application" 2011 3rd International Conference on Electronics Computer Technology (ICECT), pp. 302-306. DOI: 10.1109/ICECTECH.2011.5942103.

[24] Junsangsri, Pilin and Lombardi, Fabrizio, "Time/Temperature Degradation of Solar Cells under the Single Diode Model" 2010 IEEE 25th International Symposium on Defect and Fault Tolerance in VLSI Systems, pp. 240-248. DOI: 10.1109/DFT.2010.36.

[25] Mahmoud, Y. A., Xiao, W. and Zeineldin, H. H., "A Simple Approach to Modeling and Simulation of Photovoltaic Modules" IEEE Transactions on Sustainable Energy, Vol. 3, No. 1, pp. 185-186, 2012. DOI: 10.1109/TSTE.2011.2170776.

[26] Thang, T. V., Thao, N. M., Jang, Jong-Ho and Park, Joung-Hu, "Analysis and Design of Grid-Connected Photovoltaic Systems with Multiple-Integrated Converters and a Pseudo-DC-Link Inverter" IEEE Transactions on Industrial Electronics, Vol. 61, No. 7, pp. 3377-3386, 2014. DOI: 10.1109/TIE.2013.2281153.

[27] Yi Lei, Zhengming Zhao, Wei Xu and Jianguo Zhu, “Modeling and Analysis of MW-Level Grid-Connected PV Plant” 37th Annual Conference on IEEE Industrial Electronics Society (IECON), pp. 890-895, 2011. DOI: 10.1109/IECON.2011.6119428.

[28] Rahmani, R., Fard, M., Shojaei, A. A., Othman, M. F. and Yusof, R., “A Complete Model of Stand-alone Photovoltaic Array in MATLAB-Simulink Environment” 2011 IEEE Student Conference on Research and Development (SCOReD), pp. 46-51, 2011. DOI: 10.1109/SCOReD.2011.6148706.

[29] University of Notre Dame. The Prashant Karat Laboratory. http://www3.nd.edu/~kamatlab/images/AM_15_Solar_spectrum.jpg (Accessed 2015-5-1)

[30] Photon.info. http://www.photon.info/photon_home_en.photon (Accessed 2015-5-1)

# Vita


| | |
|---|---|
| Name | : Fahad Ibrahim Bousbait |
| Nationality | : Saudi |
| Date of Birth | : 3/9/1983 |
| Email | : fahadiab@hotmail.com |
| Address | : Dammam, Al-Shatea west district, Bakkar Al-Thaqafi Street. P.O.Box 36657, Dammam 31429, Saudi Arabia. |
| Academic Background | : Bachelor of Science in Electrical Engineering (February 2006), from King Fahd University of Petroleum & Minerals, Dhahran, Saudi Arabia. |